Angewandte Communications

Helix Inducers

DOI: 10.1002/anie.201((will be filled in by the editorial staff))

Comparative α-Helicity of Cyclic Pentapeptides in Water **

*Aline D. de Araujo,[1‡] Huy N. Hoang,[1‡] W. Mei Kok,[1] Fredrik Diness,[1¶] Praveer Gupta,[1¶] Timothy A. Hill,[1] David Price,[2] Spiros Liras,[2] David P. Fairlie[1]**

Abstract: *Helix constrained polypeptides have attracted great interest for modulating protein-protein interactions (PPI). It is not known which are the most effective helix-inducing strategies for designing PPI agonists/antagonists. Cyclization linkers (X_1-X_5) were compared here, using circular dichroism and 2D-NMR spectroscopy, for α-helix induction in simple model pentapeptides, Ac-cyclo(1,5)-[X_1-Ala-Ala-Ala-X_5]-NH_2, in water. In this very stringent test of helix induction, a Lys1→Asp5 lactam linker conferred greatest α-helicity, hydrocarbon and triazole linkers induced a mix of α- and 3_{10}- helicity, while thio- and dithio- ether linkers produced less helicity. The lactam linked cyclic pentapeptide was also the most effective α-helix nucleator attached to a 13-residue model peptide.*

Many biological processes are mediated by protein-protein interactions (PPIs), but discovering small drug-like molecules to target PPIs has been challenging due to the large polar interacting surface areas involved and only very shallow ligand-binding hydrophobic clefts.[1] PPIs often involve a protein α-helix[2] of 1-4 helical turns (4-15 amino acid residues), but corresponding synthetic peptides of these lengths do not tend to form thermodynamically stable α-helix structures in water.[3] This is because water competes with the polar amide CO-NH components of peptide backbones for hydrogen bonding, whereas three backbone CO…HN hydrogen bonds are needed to define each turn of an α-helical peptide (Fig. 1A). Thus, 7-10 helical turns are usually needed for a synthetic peptide to exhibit appreciable α-helicity in water away from a helix-stabilizing protein environment. Methods developed to stabilize synthetic peptides in α-helical structures include incorporating salt bridges, chelating metal ion clips or covalent linkages to cyclize peptide segments, or attaching helix-nucleating end groups.[2c,d] However, there is no consensus as to which is the most effective strategy for inducing α-helicity in short peptides in water and systematic comparisons are needed. The shortest native peptide sequence that can theoretically form three consecutive α-helix defining hydrogen bonds is a pentapeptide (Fig. 1A), with the terminal residues being on the same helix face for sidechain-sidechain connection to lock in an α-helical conformation. Here we use a cyclic pentapeptide scaffold, Ac-cyclo(1,5)-[X_1-Ala-Ala-Ala-X_5]-NH_2, to compare the relative effectiveness of six known cyclization linkers X_1-X_5 (Fig. 1B) reported to aid helicity in polypeptides. Despite their use in polypeptides, the central question as to which is the most effective α-helix inducer in short peptides has not been answered. Only one α-helical turn is possible in pentapeptides **1-6**, which have no helicity in water when uncyclized, so this is a very demanding test of helix induction for these linkers.

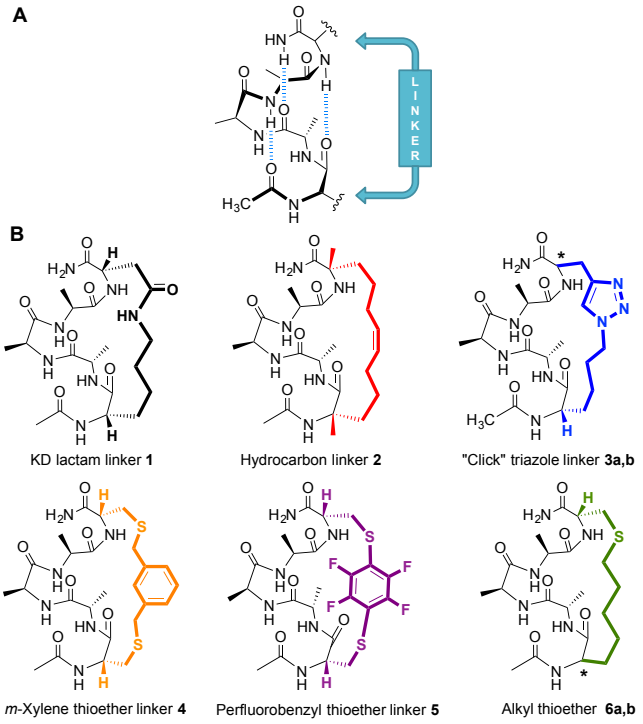

Figure 1. **A)** Three consecutive hydrogen bonds define an α-helix stabilized by linking sidechains at positions 1 and 5. **B)** Cyclic pentapeptides **1-6**. (* denotes isomers: triazole **3a**: L-, **3b**: D- at X_5; thioether **6a**,**6b**: L- or D- at X_1, see SI).

Compounds **1-6** all have three alanines, known to favor α-helicity,

[*] [1]Dr. A. D. de Araujo, Dr. H. H. Hoang, Dr. W. Mei Kok, Dr. F. Diness, Dr. P. Gupta, Dr. T. A. Hill, Prof. D. P. Fairlie
Division of Chemistry and Structural Biology
Institute for Molecular Bioscience
The University of Queensland, Brisbane, QLD 4072, Australia
Fax: +61-733462990
E-mail: d.fairlie@imb.uq.edu.au

[2]Dr. David Price, Dr. Spiros Liras
Pfizer Worldwide Research and Development, Cardiovascular, Metabolic and Endocrine Diseases, Cambridge, MA, USA

[‡] These authors contributed equally to this work.

[**] We acknowledge ARC for a Federation Fellowship to DF (FF0668733) and research funding (DP1096290, DP130100629), NHMRC for a Senior Principal Research Fellowship to DF (APP1027369) and research funding (APP511194), and Carlsberg Foundation (Denmark) for a postdoctoral fellowship to F.D.

Supporting information for this article is available on the WWW under http://dx.doi.org/10.1002/anie.201xxxxxx

between their different linkers at positions 1 and 5. Compound **1** incorporates a sidechain to sidechain lactam linker, which is a helix inducer in polypeptides,[3,4] hormones (PTH[5], GLP-1[6], nociception[7]), PPI inhibitors (HIV[8], RSV[9] viral fusion) and others[10] and in short peptides in water.[11] The position of the amide bond in the linker of **1** is known to be crucial for optimal helicity, other lactam crosslinks showing partial or no α-helicity.[11b] Compound **2** was formed by a ring-closing metathesis cyclization[12] using α,α-disubstituted amino acids with olefin tethers.[13] Such a crosslinking strategy has been used[14] for example to design helices that promote BCL2 apoptosis[14a] or inhibit HIV-1 capsid assembly[14b] or NOTCH transcription.[14c] The α-methyl groups in the linker in **2** reportedly assist helix stabilization, although may be not be essential.[14d] Compound **3** was made by Cu(I)-mediated Huisgen 1,3-dipolar cycloaddition (click reaction)[15] of azido norleucine and L- or D-propargylglycine (Pra) at i and i+4 positions, and this has been applied to biological targets like PTH[15a] and ß-catenin/BCL9.[15c] Compounds **4** and **5** were cyclized by reacting cysteine side chains with dibromo-*m*-xylene[16] or perfluoroaryl crosslinkers, respectively.[17] The thioether in **6**, not known as a helix constraint, was compared as it has no polar or ring linker atoms. Based on uses in polypeptides,[11,13,15] the linkers in Figure 1B represent the best reported helix-inducing connectivity with optimized linker size (6-, 7-, 8-, 9-atom bridges), positioning of heteroatoms, rings or double bonds, and cycle-forming D/L- amino acids.

Linear peptide precursors to **1-6** were synthesized by standard Fmoc solid-phase peptide synthesis protocols and cyclized to **1-6** by reported procedures (Supp. Info., SI). Circular dichroism spectra (Fig. 2A) recorded in phosphate buffer (pH 7.2, 298K) are typically used[18a] to quantitate relative % helicity (Figure S1, SI), based on molar ellipticity at λ = 222 nm in polypeptides (but ~215 nm in short peptides[11]). The Lys1-Asp5 lactam crosslinked peptide **1** showed strong α-helicity in water, with two symmetrical minima peaks at 207 and 215 nm (ratio 1.0: 1.1) and a positive maximum at 190 nm. Relative to **1** (100% α-helicity), hydrocarbon **2** and triazole **3a** had reduced helicity (62%) and slightly shifted minima (203 : 217 nm; 1.0 : 0.8) consistent with less α-helical structure than **1**. The triazole linker afforded more helicity when formed from click cyclization of L-Pra at position 1 (**3a**, 62%) than D-Pra (**3b**, 48%). Thioether-bridged peptides **4-6** were much less helical and less structured, with weak elipticity at λ ~215-220 nm, no maximum at ~190 nm, and a negative minimum at ~199 nm.

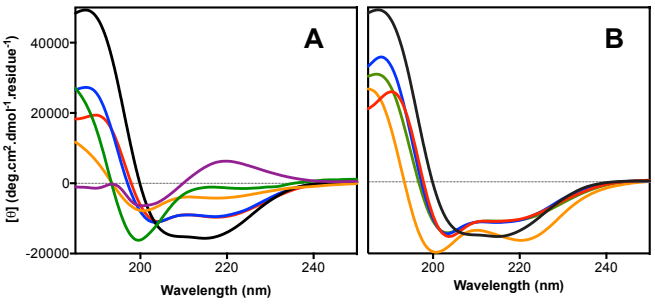

Figure 2. CD spectra of crosslinked pentapeptides: KD lactam **1** (black), hydrocarbon **2** (red), triazole **3a** (blue), *m*-xylene thioether **4** (orange), perfluorobenzyl **5** (violet) and alkyl thioether **6a** (green) at 298 K in: **A**) 10 mM phosphate buffer pH 7.2 or **B**) 50% TFE/10mM phosphate buffer pH 7.2.

To identify any further capacity for helix induction in **1-6**, CD spectra were also measured after adding the helix-promoting solvent, 2,2,2-trifluoroethanol (TFE) (Fig. 2B). The CD spectrum for **1** did not change on adding TFE, indicating maximal helicity. However, α-helicity (based on $[\theta]_{215}$) increased for **2** and **3a** from 62% to 75% (50% TFE). Of thioether linkers **4-6**, both **4** (35% to 98%) and **6a** (3% to 74%) became more helical in 50% TFE.

Linkers in **1-6** are reportedly the best of their kinds for inducing helicity in polypeptides, but there are 7 atoms in the linker in **1** versus 8 atoms in **2** and **3a**. To investigate if shortening the linker in **2** or **3** to a 7-atom bridge might increase helix stabilization in water, we prepared analogues (Fig. 3) with 7-membered hydrocarbon (**2a**,**b**) or triazole (**3c**,**d**) crosslinks. Compared to the 8-carbon linker in **2**, a 7-carbon linker induced similar helicity when the *cis*-alkene bond was at C4-C5 positions (**2b**, Fig. 3A), but no helicity when at C3-C4 (peptide **2a**) or C2-C3.[13a] Shortening the triazole linker in **3a** to a 7-atom bridge (**3c**, **3d**) was detrimental to helicity here (Figure 3B), and in longer peptides reported.[15c] Thus, helicity was very sensitive to the location of the constraint in the linker, as also reported for lactam linked analogues of **1**.[11] This is likely due to some precision needed in aligning all 6 amides in **1-3** to form 3 H-bonds in an α-helix (Fig. 1A).

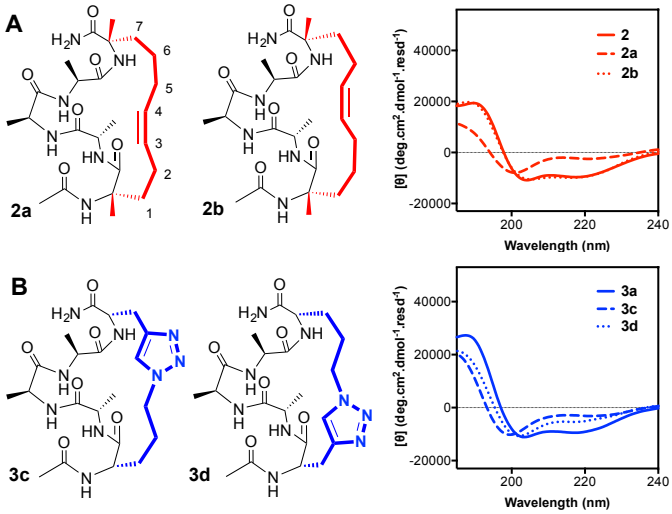

Figure 3. Cyclic pentapeptides with a 7-atom hydrocarbon (**A**) or triazole (**B**) linker and their CD spectra (10 mM phosphate buffer, pH 7.2, 298 K).

Using ^{1}H NMR spectroscopy, three dimensional solution structures were determined for **1** and **3a** (90% H_2O:10% D_2O) and **2** (40% H_2O:10% D_2O, 50% CD_3CN). We have previously reported some structural data for **1** and close analogues.[10a,11] All the peptides **1**, **2** and **3a** showed some low amide coupling constants, $^{3}J_{NHC\alpha H} < 6$ Hz (Fig. 4; Table S1, SI) consistent with some helical structure.[18b] For **1** and **3a**, all but Asp5 (**1**) and X5 (**3a**) coupling constants were < 6 Hz, consistent with helicity. For **2**, Ala3 and Ala4 had $^{3}J_{NHC\alpha H} >$ 6 Hz, indicating less helicity, consistent with CD spectra. Three consecutive low amide NH temperature coefficients (Fig. S2, S3, S4; Table S1, SI) for **1**, **2** and **3a** were consistent with three consecutive hydrogen bonds. In addition, the ROESY spectrum for **1**, **2** and **3a** showed some αN(i,i+2), αN(i,i+3) and αN(i,i+4) ROE signals indicative of helical structures (Fig. 4). However, αN(i,i+3) and αN(i,i+4) ROE intensities were stronger and more numerous for peptide **1** than **2** and **3a**, which had more αN(i,i+2) than for **1**. This suggested more α-helical structure in **1** than **2** and **3a**, and some 3_{10}-helicity in **2** and **3a**. NMR-derived solution structures for **1** (Fig. 4) showed a single α-helical turn with RSMD 3.360 Å versus an idealized α-helix, while **2** and **3a** had RMSD 3.375 Å and 3.365 Å, respectively. The Cα-Cα distance between first and fifth residues in **1**, **2** and **3a** (5.59 Å, 5.85 Å and 5.90 Å, respectively) was compared

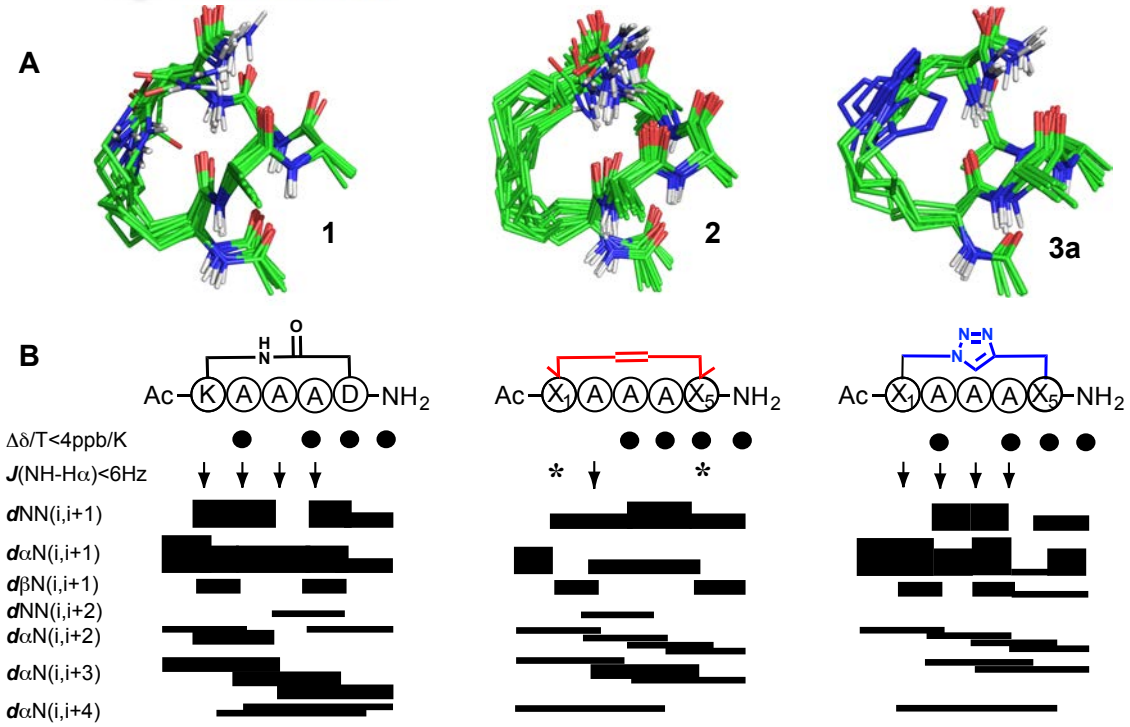

Figure 4. **A)** Superimposition of 20 lowest energy structures for cyclic pentapeptides **1**, **2** and **3a** calculated by NMR at 298 K. Average backbone RMSD for structure ensemble was 0.37, 0.49 and 0.32 Å, respectively. **B)** ROE summary diagram for **1**, **2** and **3a** showing distance restraints used to calculate the peptide structure. Bar thickness reflects the intensity of the ROE cross peaks. Asterisk indicates absence of coupling constant due to presence of α-methyl group.

to the corresponding distance in an idealized α-helix (5.51 Å, ϕ = -57°; ψ = -47°) and 3_{10}-helix (8.30 Å, ϕ = -50°; ψ = -28°). This indicated slightly more elongated (mix with 3_{10}-) helical structures in **2** and **3a**, than the more compact α-helix in **1**, consistent with CD spectra. This is also supported by Ramachandran[18c] plots (Fig. 5) obtained from the peptide structures (Fig. 4). Only for lactam **1** did all (ϕ, ψ) angles occupy space corresponding to α-helicity in the plot, whereas peptides **2** and **3a** both had several angles located outside of the Ramachandran space that defines α-helicity.

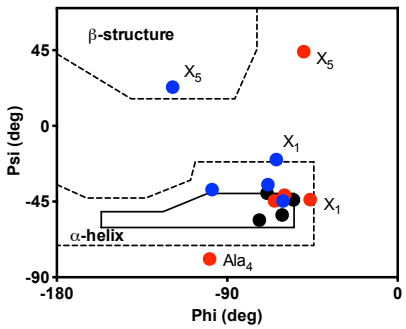

Figure 5. Ramachandran plots of (ϕ, ψ) angles derived from the average of the 20 lowest energy NMR-derived solution structures calculated for **1** (black), **2** (red) and **3** (blue). Only those for **1** are entirely in α-helix space. Solid line encloses a region allowed with full radii, dashed lines enclose regions allowed with smaller radii from hard-sphere calculations.[18c]

The unique presence of an amide bond in the linker of **1** potentially allows additional H-bonding to the backbone, which might account for greater α-helicity in **1**. However, the temperature dependence of the chemical shift for the linker amide NH in **1** ($\Delta\delta/T$ ~9.3 Hz) was much higher than is characteristic of a hydrogen bond ($\Delta\delta/T \leq 4$ Hz).[18d] Moreover, when the amide NH was replaced by a lactone O (**1a**) or amide NMe (**1c**) (Fig. 6), the molar ellipticity (θ_{215}) was unchanged, indicating no effect of removing the amide NH on α-helicity. Although molar ellipticity was unchanged at θ_{215}, the CD spectrum for lactone **1a** differs from lactam **1** by an increase in the π-π* band at 204 nm and reduced intensity of the 190 nm band, which indicates a slight relaxation of the helical structure, consistent with more 3_{10}-helix in the mix. The molar ellipticity $[\theta]_{215}$ was similarly unchanged when the linker amide NH became NMe (**1b** vs **1c**, Figure 6), consistent with the linker NH not forming a hydrogen bond to the backbone. We used Ac-cyclo(1,5)-[KLLLD]-NH_2 (**1b**) to check the effect of *N*-methylation of the lysine ε-NH due to easier synthesis.

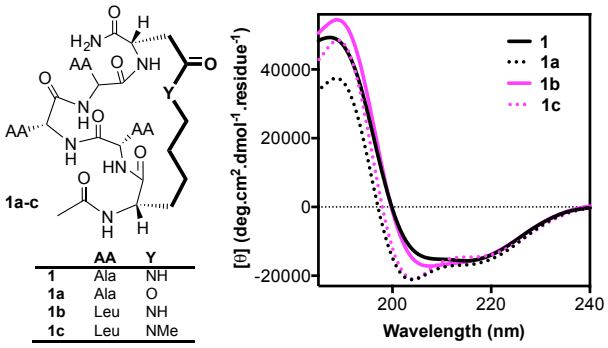

Figure 6. Lactone (**1a**) and lactam (**1b**, **1c**) linked cyclic peptide analogues of **1** and comparative CD spectra (10 mM phosphate buffer, pH 7.2, 298 K).

Having established the rank order of α-helix induction of these linkers in the shortest possible alanine-containing peptide helix, we tested the relative capacities of linkers to nucleate α-helicity in a longer peptide sequence. A series of 18mer peptides, Ac-AARAARAARAARA-[X_{14}ARAX_{18}]-NH_2 (Ala and Arg residues used to aid peptide helicity and solubilization in water), was prepared and their CD spectra were examined in aqueous media (Fig. 7). The cyclic pentapeptides **1**, **2** and **3a** substantially

increased helicity (92%; 50% and 51% respectively) when attached to the linear sequence **7** (23% helicity).

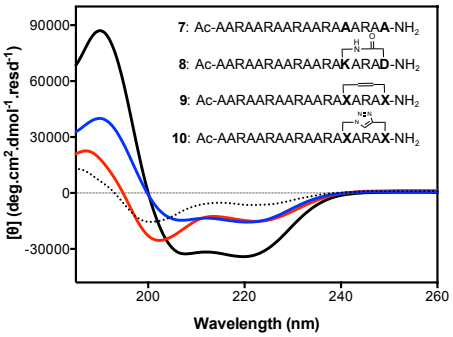

Figure 7. CD spectra of Ac-AARAARAARAARA (50 μM) attached to AARAA-NH_2 (**7**, dots), lactam **1** (**8**, black), hydrocarbon **2** (**9**, red) and triazole **3a** (**10**, blue) in 50 mM phosphate buffer (pH 7.2, 298K).

In conclusion, the Lys1→Asp5 lactam-bridge was the most effective crosslink in these cyclic pentapeptides at inducing α-helicity in water, producing the smallest and most compact helical structure for **1**. Hydrocarbon (in **2**) and triazole (in **3**) 1→5 crosslinks were also able to induce some helicity in water, but their structures were conformationally more flexible and less α-helical, as evidenced by CD and NMR spectroscopic studies. The linkers in **2** and **3** induced looser, slightly more elongated, helical structures in their conformational ensemble mix. This is not to say that **2** and **3** will be ineffective helix nucleators within longer peptides, but were assessed here under very demanding conditions in an otherwise non-helical 5-residue peptide and as helix nucleators attached to the end of a model 13-mer peptide with little helicity in water. In longer bioactive peptides already possessing some helicity in water, each of these linkers may be satisfactory for an intended use either because they aid helix formation or because they enable access to other non-alpha helical structures due to their inherent flexibility. However, in the very short peptides studied here, **1** was the most α-helical cyclic pentapeptide in water and also the most effective helix nucleator attached to a model 13-mer peptide. These findings may enable optimal selection of helix-constraining linkers in short peptides.

Received: ((will be filled in by the editorial staff))
Published online on ((will be filled in by the editorial staff))

Keywords: alpha helix • cyclic peptide • circular dichroism • NMR structure • helix induction

[1] a) D. J. Craik, D. P. Fairlie, S. Liras, D. Price, *Chem. Biol. Drug. Des.* **2013**, *81*, 136-147; b) V. Azzarito, K. Long, N. S. Murphy, A. J. Wilson, *Nat. Chem.* **2013**, *5*, 161-173.

[2] a) B. N. Bullock, A. L. Jochim, P. S. Arora, *J. Am. Chem. Soc.* **2011**, *133*, 14220-14223; b) V. Haridas, *Eur. J. Org. Chem.* **2009**, 5112-5128; 2c) E. Cabezas, A. C. Satterthwait, *J. Am. Chem. Soc.* **1999**, *121*, 3862-3875; 2d) A. Patgirl, A. L. Jochim, P. S. Arora, *Acc. Chem. Res.* **2008**, *41*, 1289-1300.

[3] a) K. Estieu-Gionnet, G. Guichard, *Expert Opinion on Drug Discovery* **2011**, *6*, 937-963; b) R. Dharanipragada, *Future Med. Chem.* **2013**, *5*, 831-849; c) L. K. Henchey, A. L. Jochim, P. S. Arora, *Curr. Op. Chem. Biol.* **2008**, *12*, 692-697; d) J. Garner, M. M. Harding, *Org. Biomol. Struct.* **2007**, *5*, 3577-3585; e) M. J. I. Andrews, A. B. Tabor, *Tetrahedron* **1999**, *55*, 11711-43.

[4] J. W. Taylor, *Biopolymers* **2002,** *66*, 49-75.

[5] M. Chorev, E. Roubini, R. L. McKee, S. W. Gibbons, M. E. Goldman, M. P. Caulfield, M. Rosenblatt, *Biochemistry* **1991,** *30*, 5968-5974.

[6] E. N. Murage, G. Gao, A. Bisello, J.-M. Ahn, *J. Med. Chem.* **2010,** *53*, 6412-6420.

[7] R. S. Harrison, G. Ruiz-Gomez, T. A. Hill, S. Y. Chow, N. E. Shepherd, R.-J. Lohman, G. Abbenante, H. N. Hoang, D. P. Fairlie, *J. Med. Chem.* **2010**, *53*, 8400-8408.

[8] a) Sia, S. K.; Carr, P. A.; Cochran, A. G.; Malashkevich, V. N.; Kim, P. S. *Proc. Natl. Acad. Sci. USA* **2002**, 99, 14664-14669; b) Mills, N. L.; Daugherty, M. D.; Frankel, A. D.; Guy, R. K. *J. Am. Chem. Soc.* **2006**, *128*, 3496-3497.

[9] N. E. Shepherd, H. N. Hoang, V. S. Desai, E. Letouze, P. R. Young, D. P. Fairlie, *J. Am. Chem. Soc.* **2006**, *128*, 13284-13289.

[10] a) R. S. Harrison *et al*,. *Proc. Natl. Acad. Sci. USA* **2010,** *107*, 11686-11691; b) T. Rao, G. Ruiz-Gomez, T. A. Hill, H. N. Hoang, D. P. Fairlie, J. M. Mason, *Plos One* **2013,** *8*, e59415.

[11] a) N. E. Shepherd, G. Abbenante, D. P. Fairlie, *Angew. Chem., Int. Ed.* **2004,** *43*, 2687-2690; b) N. E. Shepherd, H. N. Hoang, G. Abbenante, D. P. Fairlie, *J. Am. Chem. Soc.* **2005,** *127*, 2974-2983. c) N. E. Shepherd, H. N. Hoang, G. Abbenante, D. P. Fairlie. *J Am Chem Soc.* **2009**, *131*, 15877-15886.

[12] a) H. E. Blackwell, R. H. Grubbs, *Angew. Chem. Int. Ed.* **1998,** *37*, 3281-3284; b) H. E. Blackwell, J. D. Sadowsky, R. Howard, J. N. Sampson, J. A. Chao, W. E. Steinmetz, D. J. O'Leary, R. H. Grubbs, *J. Org. Chem.* **2001,** *66*, 5291-5302.

[13] a) C. E. Schafmeister, J. Po, G. L. Verdine, *J. Am. Chem. Soc.* **2000,** *122*, 5891-5892; b) G. L. Verdine, G. J. Hilinski, *Meth. Enzymol.* **2012,** *503*, 3-33.

[14] a) L. D. Walensky, A. L. Kung, I. Escher, T. J. Malia, S. Barbuto, R. D. Wright, G. Wagner, G. L. Verdine, S. J. Korsmeyer, *Science* **2004,** *305*, 1466-1470; b) H. Zhang et al, *J. Mol. Biol.* **2008**, *378*, 565-580; c) R. E. Moellering, *et al*, *Nature* **2009,** *462*,182-188; d) E. Gavathiotis et al, *Nature* **2008,** *455*, 1076-1081; e) E. S. Leshchiner, C. R. Braun, G. H. Bird, L. D. Walensky, *Proc. Natl. Acad. Sci. USA* **2013,** *110*, 303-312; f) M. L. Stewart, E. Fire, A. E. Keating, L. D. Walensky, *Nat. Chem. Biol.* **2010,** *6*, 595-601; g) T. L. Joseph, D. Lane, C. Verma, *Cell Cycle* **2010,** *9*, 4560-4568; h) C. Phillips et al, *J. Am. Chem. Soc.* **2011,** *133*, 9696-9699; i) D. O. Sviridov, I. Z. Ikpot, J. Stonik, S. K. Drake, M. Amar, D. O. Osei-Hwedieh, G. Piszczek, S. Turner, A. T. Remaley, *Biochem. Biophys. Res. Commun.* **2011,** *410*, 446-451; j) C. Phillips *et al*,*J. Am. Chem. Soc.* **2011**, *133*, 9696-99; k) Y. W. Kim, G. L. Verdine, *Bioorg. Med. Chem. Lett.* **2009**, 19, 2533-2536; l) D. J. Yeo, S. L. Warriner, A. J. Wilson, *Chem. Commun.* **2013**, *49*, 9131-9133.

[15] a) M. Scrima, A. Le Chevalier-Isaad, P. Rovero, A. M. Papini, M. Chorev, A. M. D'Ursi, *Eur. J. Org. Chem.* **2010,** *73*, 446-457; b) A. Al Temimi, R. M. J. Liskamp, D. T. S. Rijkers, *J. Pept. Sci.* **2012,** *18*, S184-S185; c) S. A. Kawamoto, A. Coleska, X. Ran, H. Yi, C.-Y. Yang, S. Wang, *J. Med. Chem.* **2012,** *55*, 1137-1146; d) S. Cantel, C. I. A. Le, M. Scrima, J. J. Levy, R. D. DiMarchi, P. Rovero, J. A. Halperin, A. M. D'Ursi, A. M. Papini, M. Chorev, *J. Org. Chem.* **2008,** *73*, 5663-5674.

[16] H. Jo, N. Meinhardt, Y. Wu, S. Kulkarni, X. Hu, K. E. Low, P. L. Davies, W. F. DeGrado, D. C. Greenbaum, *J. Am. Chem. Soc.* **2012**, *134*, 17704-17713.

[17] A. M. Spokoyny, Y. Zou, J. J. Ling, H. Yu, Y.-S. Lin, B. L. Pentelute, *J. Am. Chem. Soc.* **2013,** *135*, 5946-5949.

[18] a) P. Z. Luo, R. L. Baldwin, *Biochemistry* **1997**, *36*, 8413-8421; b) A. Pardi, M. Billeter, K. Wuthrich, *J. Mol. Biol.* **1984**, *180*, 741-751; c) G. N. Ramachandran, V. Sasikharan, *Adv. Protein. Chem.* **1968**, *23*, 283-438; d) D. S. Wishart, B. D. Sykes, F. M. Richards, *Biochemistry* **1992**, *31*, 1647-1651.

Helix Inducers

Aline D. de Araujo,[1‡] Huy N. Hoang,[1‡] W. Mei Kok,[1] Fredrik Diness,[1] Praveer Gupta,[1] Timothy A. Hill,[1] David Price,[2] Spiros Liras,[2] David P. Fairlie[1]*_____ **Page – Page**

Comparative α-Helicity of Cyclic Pentapeptides in Water **

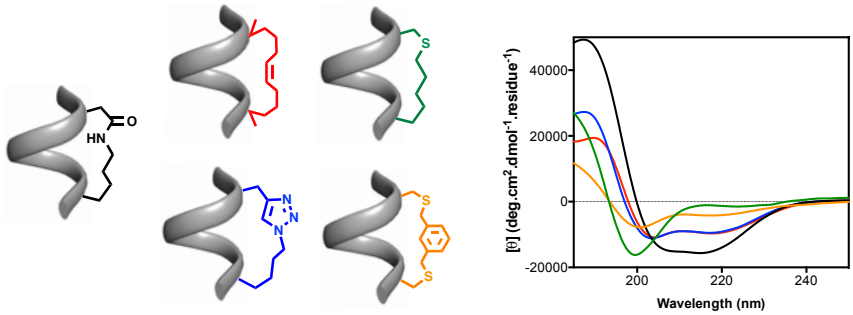

Covalent linkers between amino acid sidechains in peptide sequences can induce bioactive α–helical conformations that modulate protein-protein interactions. A lactam linker is shown here to confer greatest α-helicity in water to a cyclic pentapeptide, forming a near idealized one-turn α-helix, while other crosslinks induced a mix of α- and 3_{10}- helicity or negligible helicity. The lactam-linked cyclic pentapeptide was also the most effective α-helix nucleator when attached to a 13-residue alanine-rich peptide in water.

Angewandte Communications

SUPPORTING INFORMATION

Comparative α-Helicity of Cyclic Pentapeptides in Water

*Aline D. de Araujo,[1‡] Huy N. Hoang,[1‡] W. Mei Kok,[1] Fredrik Diness,[1] Praveer Gupta,[1] Timothy A. Hill,[1] David Price,[2] Spiros Liras,[2] David P. Fairlie[1]**

[1]Division of Chemistry and Structural Biology, Institute for Molecular Bioscience, The University of Queensland, Brisbane, QLD 4072, Australia.

[2]Pfizer Worldwide Research and Development, Cardiovascular, Metabolic and Endocrine Diseases Medicinal Chemistry, Cambridge, Massachusetts and Groton, Connecticut, USA

EXPERIMENTAL PROCEDURES

Abbreviations

Alloc, allyloxyxarbonyl; DBU, 1,8-Diazabicyclo[5.4.0]undec-7-ene; DIPEA, diisopropylethylamine; DMAP, 4-dimethylaminopyridine; DMF, dimethylformamide; ESI-MS, electrospray ionization mass spectrometry; Fmoc, 9-fluorenylmethyloxycarbonyl; HBTU, 2-(1*H*-benzotriazol-1-yl)-1,1,3,3-tetramethyl uronium hexafluorophosphate: HCTU, 2-(1*H*-6-chlorobenzotriazol-1-yl)-1,1,3,3-tetramethyl uronium hexafluorophosphate; HR-MS, High-resolution mass spectroscopy; MBHA, 4-methyl-benzylhydrylamine; Mmt, 4-methoxyltrityl; MTBD, 7-methyl-1,5,7-triazabicyclo[4.4.0]dec-5-ene; Mtt, 4-methyltrityl; NBS, nitrobenzenesulfonyl; PyBOP, benzotriazol-1-yl-oxytripyrrolidinophosphonium hexafluorophosphate; RP-HPLC, reserved-phase high performance liquid chromatography; RP-HPLC; UHPLC, reserved-phase ultra high performance liquid chromatography; OPip, phenyl isopropyl ester; RT, room temperature; SPPS, solid-phase peptide synthesis; *t*Bu, *tert*-butyl; TFA, trifluoroacetic acid; TFE, 2,2,2-trifluoroethanol; TIS, triisopropylsilane; Trt, triphenylmethyl.

Materials

All solvents and reagents used during peptide chain assembly were peptide synthesis grade and purchased from commercial suppliers unless otherwise stated.

General manual SPPS of the pentapetide linear precursors

Short pentapeptides were prepared by standard manual Fmoc solid-phase synthesis using HBTU as coupling reagent and Rink Amide MBHA resin.[1] A 4-fold excess of the respective protected amino acid was activated using HBTU (4 equiv) and DIPEA (4 equiv) in DMF and coupled to the resin for 10 minutes. Fmoc deprotections were achieved by 2 × 1 min treatments with excess (1:1) piperidine:DMF. Coupling yields were monitored by ninhydrin test. The *N*-terminus was acetylated with Ac_2O:DIPEA:DMF (0.87:0.47:15 mL) for 10 minutes.

General automated SPPS for the synthesis of the longer peptides

Peptides **7**-**10** were assembled on a peptide synthetizer (Symphony) using Rink Amide MBHA resin. 5 equiv. of Fmoc-protected amino acid, 5 equiv. of HCTU and 5 equiv. of DIPEA were used in 2 x 15min coupling cycles. Fmoc deprotections

were achieved by 2 × 3 min treatments with excess 2:1 piperidine:DMF. The *N*-terminus was acetylated with Ac_2O:DIPEA (2:1) in DMF for 10 minutes Details on the C-terminal cyclization is described for each individual peptide in the next pages.

Cleavage from solid support and peptide purification

Peptides were cleaved from the resin by treatment with TFA:TIS:H_2O (95:2.5:2.5) for 2 h. The crude peptides were precipitated and washed with cold Et_2O, redissolved in 50% acetonitrile/0.05% TFA in water and lyophylised. Peptides were purified by RP-HPLC using a Phenomenex Luna C18 column eluting at a flow rate of 20 mL/min and a gradient of 0 to 50% buffer B (90% CH_3CN/10% H_2O/0.1% TFA in buffer A, 0.1% TFA in water) over 30 minutes.

Analytical methods

Analytical RP-HPLC was performed on an Agilent system, using a Phenomenex Luna C18 5 um (250 x 4.60 mm) column eluting at flow rate of 1 mL/min and gradient 0 to (x) % buffer B (90% CH_3CN/10% H_2O/0.1% TFA in buffer A, 0.1% TFA in water) over 20 minutes. Analytical UHPLC was performed on a Shimadzu Nexre using Agilent Zorbax R-ODS III column 2.0 mm i.d x 75 mm 1.6 mm). High-resolution mass spectroscopy was conducted on an Applied Biosystems QSTAR Elite time-of-flight spectrometer.

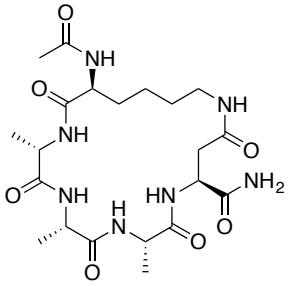

Lactam cyclopentapeptide Ac-(1,5)-[KAAAD]-NH_2 (1)

Fmoc-Lys(Mtt)-OH and Fmoc-Asp(OPip)-OH were employed for incorporation of non-standard amino acids at positions 1 and 5 respectively.[1] The peptide Ac-Lys(Mtt)-Ala-Ala-Ala-Asp(OPip) was assembled on the solid support as described in the general procedure. The resin was then washed with DCM and treated repeatedly with 2% TFA in DCM (5 x 2 min). After washing with DMF, a solution of PyBOP (4 equiv) and DIPEA (4 equiv) in DMF was added to the resin and the reaction was agitated overnight. Subsequently, the peptide was cleaved by TFA acidolysis and purified by RP-HPLC. Analytical data identical to that previously reported.[1]

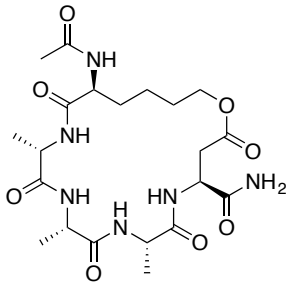

Lactone cyclopentapeptide (1a)

Boc-L-6-hydroxynorleucine and Fmoc-Asp(OPip)-OH were employed for incorporation of non-standard amino acids at positions 1 and 5 respectively. The peptide Boc-(6-hydroxynorleucine)-Ala-Ala-Ala-Asp(OPip) was assembled on the solid support as described in the general procedure. The cyclization step was carried out as follow: first, the resin was treated with 2% TFA in DCM (10 x 2 min), washed with DMF and then a solution of PyBOP (2 equiv), DMAP (1 equiv) and DIPEA (1 equiv) in DMF was added to the resin and the reaction was stirred overnight. The cyclic peptide was cleaved by TFA acidolysis and the crude material was isolated after precipation with diethylether. The crude was dissolved in a minimal of DMF and the N-terminal acetylated with Ac_2O (4 equiv) and DIPEA (4 equiv) for 30 min. The solvent was removed in high vacuum and the resulting solid was redissolved in acetonitrile. The final product was purified by RP-HPLC.

Analytical HPLC: linear gradient from 0% to 30% B over 20 min, R_t = 14.2 min. HR-MS for $[M+H]^+$: 499.2511; (calculated for **1a**: 499.2511).

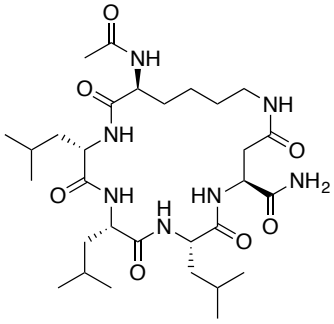

Lactam cyclopentapeptide Ac-(1,5)-[KLLLD]-NH_2 (1b)

Fmoc-Lys(Mtt)-OH and Fmoc-Asp(OPip)-OH were employed for incorporation of non-standard amino acids at positions 1 and 5 respectively.[1] The peptide Ac-Lys(Mtt)-Leu-Leu-Leu-Asp(OPip) was assembled on the solid support as described in the general procedure. The resin was then washed with DCM and treated repeatedly with 2% TFA in DCM (5 x 2 min). After washing with DMF, a solution of PyBOP (4 equiv) and DIPEA (4 equiv) in DMF was added to the resin and the reaction was agitated overnight. Subsequently, the peptide was cleaved by TFA acidolysis and purified by RP-HPLC.

Analytical UHPLC: linear gradient from 0% to 100% B over 6 min, R_t = 3.6 min. HR-MS for $[M+H]^+$: 624.4075; (calculated for **1b**: 624.4079).

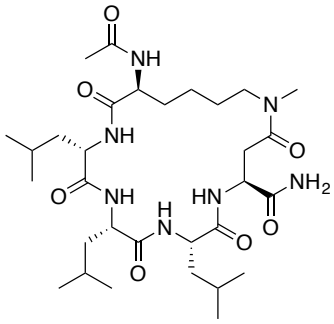

Lactam cyclopentapeptide Ac-(1,5)-[K(ε-NMe)LLLD]-NH_2 (1c)

Fmoc-Lys(Alloc)-OH and Fmoc-Asp(OPip)-OH were employed for incorporation of non-standard amino acids at positions 1 and 5 respectively. The peptide Ac-Lys(Alloc)-Leu-Leu-Leu-Asp(OPip) was assembled on the solid support as described in the general procedure. The Alloc protecting group was removed by treating the resin with a solution of phenylsilane (24 equiv) and $Pd(PPh_3)_4$ (0.1 equiv). N_2 was bubbled through the reaction mixture for 10 min and the resin was washed with DCM. A solution of 2- nitrobenzenesulfonyl chloride (4 equiv) and DIPEA (4 equiv) in DCM was added to the resin-bound free-amine peptide and shaken for 30 min. The resin was filtered and washed with DCM and DMF. The N-methylation procedure was conducted by treatment with a solution of methyl iodide (4 equiv) and MTBD (6 equiv), and the reaction was agitated overnight. For subsequent *o*-NBS deprotection, the peptide was treated with a solution of mercaptoethanol (10 equiv) and DBU (3 equiv) in DMF for 5 min. The deprotection procedure was repeated and the resin washed with DMF (5x). The resin was then washed with DCM and treated repeatedly with 2% TFA in DCM (5 x 2 min). Subsequently, the peptide was cleaved by TFA acidolysis to afford the crude linear peptide. The linear peptide was then treated with a solution of PyBOP (4 equiv) and DIPEA (4 equiv) in DMF, with overnight stirring. The reaction mixture was reduced *in vacuum* and the crude cyclized peptide was redissolved in 50% acetonitrile in H_2O and purified by RP-HPLC.

Analytical HPLC: linear gradient from 0% to 100% B over 30 min, R_t = 18.6 min. HR-MS for $[M+H]^+$: 638.4238 (calculated 638.4236).

Hydrocarbon stapled cyclopentapeptide (2)

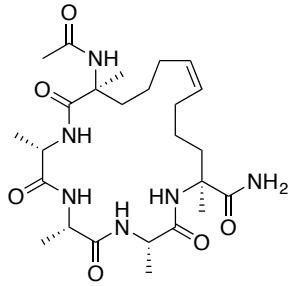

Fmoc-(S)-2-(4-pentenyl)alanine (Fmoc-X-OH) was employed for incorporation of non-standard amino acids at positions 1 and 5. The peptide Ac-X-Ala-Ala-Ala-X was assembled on the solid support as described in the general procedure. The peptide was cleaved from the resin and, after freeze-drying, submitted to cyclization. The ring-closing metathesis was performed by dissolving the crude peptide (23mg, 0.0437mmol) in DCM (55 mL), followed by addition of Grubb's catalyst 1st generation (22mg) under argon.[2] After 5 h, the reaction mixture was concentrated in vacuum and the crude peptide was redissolved in 50% acetonitrile in H_2O and purified by RP-HPLC.

Analytical HPLC: linear gradient from 0% to 50% B over 20 min, R_t =19.6 min. HR-MS for $[M+H]^+$: 523.3241 (calculated for $C_{25}H_{43}N_6O_6$: 523.3239).

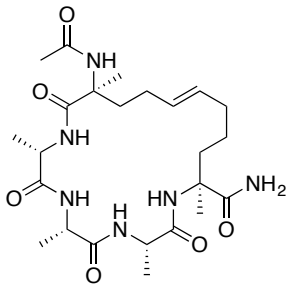

Hydrocarbon stapled cyclopentapeptide (2a)

Fmoc-(S)-2-(4-butenyl)alanine (Fmoc-Z-OH) was employed for incorporation of non-standard amino acids at position 1 and Fmoc-(S)-2-(4-pentenyl)alanine (Fmoc-Y-OH) was employed for incorporation of non-standard amino acids at position 5. The peptide Ac-Z-Ala-Ala-Ala-Y was assembled on the solid support as described in the general procedure. RCM cyclization and final purification was performed as described for peptide **2**.

For **2a**, analytical HPLC: linear gradient from 0% to 50% B over 20 min, R_t =18.1 min. HR-MS for $[M+H]^+$: 509.3081 (calculated for $C_{24}H_{41}N_6O_6$: 509.3082).

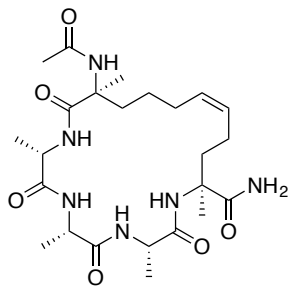

Hydrocarbon stapled cyclopentapeptide (2b)

Fmoc-(S)-2-(4-pentenyl)alanine (Fmoc-Y-OH) was employed for incorporation of non-standard amino acids at position 1 and Fmoc-(S)-2-(4-butenyl)alanine (Fmoc-Z-OH) was employed for incorporation of non-standard amino acids at position 5. The peptide Ac-Y-Ala-Ala-Ala-Z was assembled on the solid support as described in the general procedure. RCM cyclization and final purification was performed as described for peptide **2**.

For **2b**, analytical HPLC: linear gradient from 0% to 50% B over 20 min, R_t =18.2 min. HR-MS for

$[M+H]^+$: 509.3081 (calculated for $C_{24}H_{41}N_6O_6$: 509.3082).

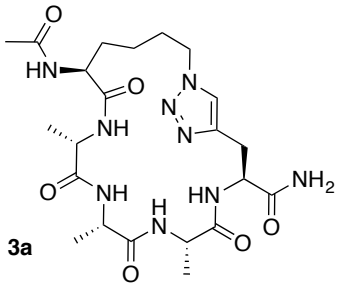

3a

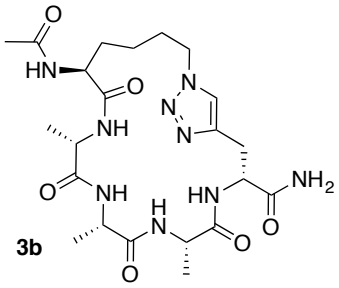

3b

Triazole stapled cyclopentapeptide (3a and **3b)**

Fmoc-Lys(N_3)-OH (Fmoc-azidolysine) and Fmoc-Pra-OH (Fmoc-L-propargylglycine for **3a**; Fmoc-D-propargylglycine for **3b**) were employed for incorporation of non-standard amino acids at positions 1 and 5 respectively. The peptide Ac-Lys(N_3)-Ala-Ala-Ala-Pra was assembled on the solid support as described in the general procedure. The peptide was cleaved from the resin and, after freeze-drying, submitted to cyclization. The crude linear peptide (24mg, 0.046mmol) was dissolved in a solution of H_20:*t*BuOH (2:1, 180 mL) containing $CuSO_4.5H_2O$ (120mg).[3] Sodium ascorbate (96mg) was added, the reaction mixture was stirred for 15 minutes, and finally quenched by addition of TFA until the solution was clear. The resulting solution was lyophilised and the cyclic product was purified by RP-HPLC.

Analytical HPLC: linear gradient from 0% to 35% B over 20 min, R_t = 15.0 min (**3a**); 14.9 min (**3b**). HR-MS for $[M+H]^+$ for **3a**: 522.2783 (calculated for $C_{22}H_{36}N_9O_6$: 522.2783); $[M+H]^+$ for **3b**: 522.2783 (calculated for $C_{22}H_{36}N_9O_6$: 522.2783).

Triazole stapled cyclopentapeptide (3c)

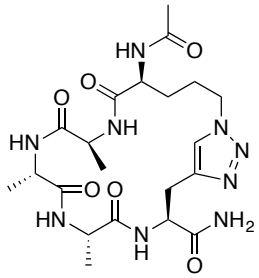

Fmoc-Orn(N_3)-OH (Fmoc-azido-ornithine) and Fmoc-Pra-OH were employed for incorporation of non-standard amino acids at positions 1 and 5 respectively. The peptide Ac-Orn(N_3)-Ala-Ala-Ala-Pra was assembled on the solid support as described in the general procedure. Cu-catalyzed click cyclization and final purification was performed as described for peptide **3a**.

For **3a**, analytical HPLC: linear gradient from 0% to 50% B over 20 min, R_t = 9.5 min. HR-MS for $[M+H]^+$: 508.2628 (calculated for $C_{21}H_{34}N_9O_6$: 508.2627).

Triazole stapled cyclopentapeptide (3d)

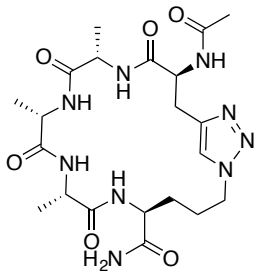

Fmoc-Pra-OH and Fmoc-Orn(N_3)-OH (Fmoc-azido-ornithine) were employed for incorporation of non-standard amino acids at positions 1 and 5 respectively. The peptide Ac-Pra-Ala-Ala-Ala-Orn(N_3) was assembled on the solid support as described in the general procedure. Cu-catalyzed click cyclization and final purification was performed as described for peptide **3a**.

For **3b**, analytical HPLC: linear gradient from 0% to 50% B over 20 min, R_t = 10.0 min. HR-MS for $[M+H]^+$: 508.2628 (calculated for $C_{21}H_{34}N_9O_6$: 508.2627).

***m*-Xylene bridged cyclopentapeptide (4)**

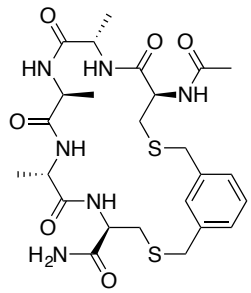

Fmoc-Cys(Mmt)-OH was used for the incorporation of cysteines at positions 1 and 5. The linear peptide Ac-Cys(Mmt)-Ala-Ala-Ala-Cys(Mmt) was assembled on the solid support as described in the general procedure. The resin was then washed with DCM and the Mmt protecting group was removed by treating the resin 1% TFA in DCM for 15 min. On-resin cyclization was conducted with α,α'-dibromo-*m*-xylene (2 eq) and DIPEA (4 eq) in DMF for 3 h at room temperature.[4] Subsequently, the peptide was cleaved by TFA acidolysis and purified by RP-HPLC.

Analytical UHPLC: linear gradient from 0% to 100% B over 6 min, R_t = 4.5 min. HR-MS for $[M+H]^+$: 581.2211 (calculated for $C_{25}H_{37}N_6O_6S_2$: 581.2211)

Tetrafluorobenzyl bridged cyclopentapeptide (5)

Fmoc-Cys(Mmt)-OH was used for the incorporation of cysteines at positions 1 and 5. The linear peptide Ac-Cys(Mmt)-Ala-Ala-Ala-Cys(Mmt) was assembled on the solid support as described in the general procedure. The resin was then washed with DCM and the Mmt protecting group was removed by treating the resin 1% TFA in DCM for 15 min. On-resin cyclization was

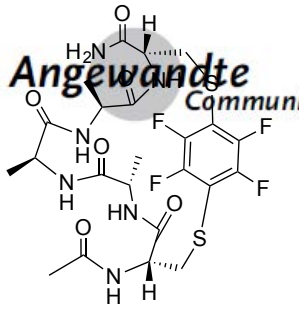

conducted with 1,4-dibromo-2,3,5,6-tetrafluorobenzene (2 eq) and DIPEA (4 eq) in DMF for 3 h at room temperature. Subsequently, the peptide was cleaved by TFA acidolysis and purified by RP-HPLC.
ESI-MS for $[M+H]^+$: 625.1 (calculated for $C_{23}H_{29}N_6O_6S_2$: 625.1).

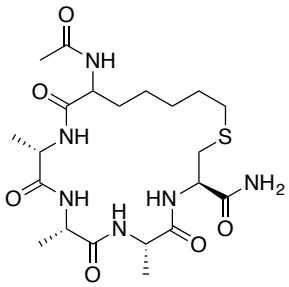

Thioether bridged cyclopentapeptide (6a and 6b)
The amino acid 2-acetamido-6-bromohexanoic acid was synthesized accordingly with a procedure reported in the literature[5] as a racemic mixture of D- and L- isomers. The racemic amino acid was used for the incorporation of non-standard residue at position 1. Fmoc-Cys(Trt)-OH was used for incorporation of cysteine at position 5. The linear peptide was assembled on the solid support as described in the general procedure. The peptide was cleaved from the resin and purified by HPLC to give two separable diastereoisomers. Each of these isomers was submitted to cyclization. The pure linear peptide (50mg, 0.086mmol) was dissolved in 50% acetonitrile (100mL) and the resulting solution was diluted in 0.1 M sodium phosphate pH 9 (350 mL). After stirring for 4 hours at room temperature, the reaction was acidified by addition of TFA, diluted twice with water and purified by RP-HPLC. The two resulting thioether cyclic products **6a** and **6b** were analyzed as cyclic thioethers. Compound **6a** was the first eluting peptide during HPLC analysis. Because both compounds showed no relevant helical conformation in water accordingly to CD analysis (Figure S1), we were not persuaded to carry on any further determination of the stereochemistry in position 1.
Analytical HPLC: linear gradient from 0% to 50% B over 20 min, R_t =13.4 min (**6a**); 0% to 35% B over 20 min, R_t =18.9 min (**6b**).
HR-MS: $[M+H]^+$ for **6a:** 501.2491 (calculated for $C_{21}H_{37}N_6O_6S$: 501.2490); $[M+H]^+$ for **6b:** 501.2490 (calculated for $C_{21}H_{37}N_6O_6S$: 501.2490).

Ac-AARAARAARAARAAARAA-NH_2 (7)
Linear peptide assembled on Symphony synthesizer, cleaved from the resin and purified following the general procedure.
Analytical UHPLC: linear gradient from 0% to 100% B over 11 min, R_t = 3.25 min. ESI-MS for $[M+ 3H]^{+3}$: 622.75 (calculated for **7**: 622.70). Full analytical data for this compound will be reported by us elsewhere.

Ac-(cyclo-14-18)-AARAARAARAARA[KARAD]-NH_2 (8)
The peptide Fmoc-Lys(Mtt)-Ala-Ala-Ala-Asp(OPip) was assembled on the solid support on a Symphony synthetizer as described in the automated general procedure. The cyclization step was carried out as follow: first, the resin was treated with 2% TFA in DCM (10 x 2 min), washed with DMF and then a solution of PyBOP (4 equiv) and DIPEA (4 equiv) in DMF was added to the resin and the reaction was stirred overnight. After washing with DMF, the N-terminal Fmoc group was removed as usual and the peptide chain was further elongated. Cleavage from the resin and purification followed the general procedure.
Analytical UHPLC: linear gradient from 0% to 100% B over 8 min, R_t = 2.60 min. ESI-MS for $[M+ 3H]^{+3}$: 616.70; (calculated for **8**: 616.71).). Full analytical data for this compound will be reported by us elsewhere.

Ac-(cyclo-14,18)-AARAARAARAARA[X_{14}-ARA-X_{18}]-NH_2, hydrocarbon linker (9)
Fmoc-(S)-2-(4-pentenyl)alanine (Fmoc-X-OH) was employed for incorporation of non-standard amino acids at positions 14 and 18. The peptide sequence Fmoc-X-Ala-Ala-Ala-X was assembled on the solid support on a Symphony synthetizer as described in the automated general procedure. The RCM was carried out in DCM and addition of Grubb's catalyst 1st generation. After washing with DMF, the N-terminal Fmoc group was removed as usual and the peptide chain was further elongated. Cleavage from the resin and purification followed the general procedure.
Analytical UHPLC: linear gradient from 0% to 100% B over 6 min, R_t = 2.60 min. ESI-MS for $[M+ 3H]^{+3}$: 624.96 (calculated for **9**: 624.94).

Ac-(cyclo-14,18)-AARAARAARAARA[X_{14}-ARA-X_{18}]-NH_2, triazole linker (10)

Fmoc-Lys(N_3)-OH and Fmoc-Pra-OH were employed for incorporation of non-standard amino acids at positions 14 and 18 respectively. The peptide sequence Ac-AARAARAARAARA-Lys(N_3)-AAA-Pra was assembled on the solid support on a Symphony synthesizer as described in the automated general procedure. The peptide was cleaved from the resin and, after freeze-drying, submitted to cyclization. The crude linear peptide (29mg) was dissolved in a solution of H_20:*t*BuOH (2:1, 150 mL) containing $CuSO_4.5H_2O$ (40mg). Sodium ascorbate (33mg) was added, the reaction mixture was stirred for 25 minutes, and finally quenched by addition of TFA until the solution was clear. The resulting solution was lyophilised and the cyclic product was purified by RP-HPLC.
Analytical HPLC: linear gradient from 0% to 60% B over 20 min, R_t = 13.1 min. ESI-MS for $[M+ 2H]^{+2}$, $[M+ 3H]^{+3}$ and $[M+ 4H]^{+4}$: 936.2, 624.8 and 468.8 respectively; (calculated for **9**: 936.0, 624.4 and 468.5 respectively).

Circular Dichroism Spectroscopy
Peptide solutions were prepared from aqueous peptide stock solutions of accurate molecular concentrations determined by NMR. The final concentration of the peptide samples was 250 μM in a) 10mM phosphate buffer pH 7.2; or b) 10mM phosphate buffer pH 7.2 in 50% TFE. CD measurements were performed using a Jasco model J-710 spectropolarimeter which was routinely calibrated with (1*S*)-(+)-10-camphorsulfonic acid. Spectra were recorded at room temperature (298K), with a 0.1 cm Jasco quartz cell over the wavelength range 260-185 nm at 50 nm/min, with a bandwidth of 1.0 nm, response time of 1 s, resolution step width of 1 nm and sensitivity of 20-50 Mdeg. Each spectrum represents the average of 5 scans. Spectra were analysed using the spectral analysis software and smoothed using 'adaptive smoothing' function. Concentrations were determined using the PULCON method.[6] NMR solutions were prepared with 540 μL of stock solution and 60 μL of D_2O. 90° pulses were accurately determined and then 1D Spectra were acquired using the standard watergate sequence with a ns= 32-64, d1= 25-35s. Spectra were also acquired for a 4.76 mM solution of L-histidine as the reference standard. The fully resolved, most downfield amide resonance was integrated and used to calculate the concentration from the equation:

$$c_u = c_R \frac{S_U T_U \vartheta^U_{360} n_R r g_R}{S_R T_R \vartheta^R_{360} n_U r g_U}$$

where *c* is the concentration, *S* is the integral(in absolute units)/number of protons, *T* is the temperature in Kelvin, θ_{360} is the 360° rf pulse, *n* is the number of scans, and *rg* is the receiver gain used for measuring the reference (R) and unknown (U) samples.

Percentage Helicity of peptides were calculated from residue-molar elipticity at 215 nm (for **1**-**6**) and at 222 nm (for longer peptides **7**-**10**) using the following equation:

$$f_{helix} = \frac{[\theta]_{222} - [\theta]_0}{[\theta]_{max} - [\theta]_0}$$

Where $[\theta]_{max}$ ($[\theta]_{max} = [\theta]_\infty(n - x)/n$) is the maximum theoretical mean residue ellipticity for a helix of n residues, $[\theta]_\infty$ is the mean residue ellipticity of an infinite helix, and x is an empirical constant that can be interpreted as the effective number of amides missing as a result of end effects, usually about 2.4-4 (we used x=3) and $[\theta]_\infty$ = (-44000 + 250T) (T is temperature of the peptide solution in ˚C). $[\theta]_0$ is the mean residue ellipticity of the peptide in random coil conformation and equals to (2220 – 53T) and $[\theta]_{222}$ ($[\theta]_{222} = 1/n \cdot [\theta_{obs}]/(10 \times l \times C)$) is the observed residue ellipticity of peptide at 222 nm. Where θ_{obs} = measured ellipticity in mdeg; n = number of peptide residues; C = sample concentration (mol/L); l = optical path length of the cell in cm.[7]

Proton NMR Spectroscopy
The samples for the NMR analyses of **1**, **2** and **3a** were prepared by dissolving the peptide (2.2 mg) in 540 μL H_2O and 60 μL D_2O at pH 5.0. 1D and 2D ^{1}H-NMR spectra were recorded on a Bruker Avance DRX-600 spectrometer. 2D ^{1}H-spectra were recorded in phase-sensitive mode using time-proportional phase incrementation for quadrature detection in the *t*1 dimension. The 2D experiments included TOCSY (standard Bruker mlevgpph pulse program), ROESY (standard Bruker roesygpph pulse program) and dqfCOSY (standard Bruker dqfcosygpph pulse program). TOCSY spectra were acquired over 6887 Hz with 4096 complex data points in *F2*, 512 increments in *F1* and 32 scans per increment. ROESY spectra were acquired over 6887 Hz with 4096 complex data points in *F2*, 512 increments in *F1* and 32 scans per increment. TOCSY and ROESY

spectra were acquired with several isotropic mixing times of 80, 100 ms for TOCSY and 350 ms for ROESY. For all NMR experiments, water suppression was achieved using modified WATERGATE. For 1D ^{1}H NMR spectra acquired in H_2O/D_2O (9:1), the water resonance was suppressed by low power irradiation during the relaxation delay (1.5 to 3.0 s). The variable NMR experiments were performed over the range of 278-318K. Spectra were processed using Topspin (Bruker, Germany) software and ROE intensities were collected manually. The *t*1 dimensions of all 2D spectra were zero-filled to 1024 real data points with 90˚ phase-shifted QSINE bell window functions applied in both dimensions followed by Fourier transformation and fifth order polynomial baseline correction. ^{1}H chemical shifts were referenced to DSS (δ 0.00 ppm) in water. $^{3}J_{NHCH\alpha}$ coupling constants were measured from 1D ^{1}H NMR and dqf-COSY spectra using XPLOR program. ^{13}C spectra were obtained with a sweep width of 20840 Hz with 20000-10000 scans and 65K data points. ^{13}C NMR spectra were ^{1}H-decoupled. Phase sensitive HSQC spectra were obtained with 900 increments in F1, 2K data points in F2 and 32 scans per increment. These were a 2-D ^{1}H/^{13}C correlation via double inept transfer using sensitivity improvement with standard Bruker pulse programs of invietgssi or invietgpsi. HMBC spectra were obtained with 1024 increments in F1, 2K data points in F2 and 32 scans per increment using a standard Bruker pulse program inv4gslprnd. There was also ^{1}H/^{13}C correlation via heteronuclear zero and double quantum coherence. The experiments were optimized on long range couplings with low-pass J-filter to suppress one bond correlations and using gradient pulses for selection.

Structure Calculations

The distance restraints used in calculating the structure for **1, 2** and **3a** in water were derived from ROESY spectra (recorded at 298K) using mixing time of 350ms with 9 and 25 ROEs for 1 and 2 respectively. ROE cross-peak volumes were classified manually as strong (upper distance constraint ≤ 2.7Å), medium (≤ 3.5Å), weak (≤ 5.0Å) and very weak (≤ 6.0Å). Standard pseudoatom distance corrections[8] were applied for non-stereospecifically assigned protons. To address the possibility of conformational averaging, intensities were classified conservatively and only upper distance limits were included in the calculations to allow the largest possible number of conformers to fit the experimental data. Backbone dihedral angle restraints were inferred from $^{3}J_{NHCH\alpha}$ coupling constants in 1D spectra, ϕ was restrained to –65 ± 30° for $^{3}J_{NHCH\alpha}$ ≤ 6Hz and to -120± 30° for $^{3}J_{NHCH\alpha}$ ≥ 8Hz. There was clearly no evidence at all for *cis*-amides about peptide bonds (i.e. no CHα-CHα (*i*, *i+1*) ROEs) in the ROESY spectra (in both 9:1 H_2O/D_2O and 100% D_2O) so all ψ-angles were set to *trans* (ψ = 180˚). Starting structures with randomised ϕ and ψ angles and extended side chains were generated using an *ab initio* simulated annealing protocol. The calculations were performed using the standard forcefield parameter set (PARALLHDG5.2.PRO) and topology file (TOPALLHDG5.2.PRO) in XPLOR-NIH with in house modifications to generated lactam bridges between lysine and aspartic acid residues. Refinement of structures was achieved using the conjugate gradient Powell algorithm with 4000 cycles of energy minimisation and a refined forcefield based on the program CHARMm.[7] Structures were visualised with InsightII and analysed for distance (>0.2Å) and dihedral angle (>5^{o}) violations using noe.inp files. Final structures contained no distance violations (>0.2Å) or angle violations (>5^{o}).

References

1. Harrison, R. S.; Ruiz-Gomez, G.; Hill, T. A.; Chow, S. Y.; Shepherd, N. E.; Lohman, R.-J.; Abbenante, G.; Hoang, H. N.; Fairlie, D. P. *J. Med. Chem.* **2010**, *53*, 8400. Harrison, R. S.; Shepherd, N. E.; Hoang, H. N.; Ruiz-Gomez, G.; Hill, T. A.; Driver, R. W.; Desai, V. S.; Young, P. R.; Abbenante, G.; Fairlie, D. P. *Proc. Natl. Acad. Sci. USA* **2010,** *107*, 11686-11691.

2. Kim, Y.-W.; Grossmann, T. N.; Verdine, G. L., *Nature Protocols* **2011,** *6* (6), 761-771

3. Kawamoto, S. A.; Coleska, A.; Ran, X.; Yi, H.; Yang, C.-Y.; Wang, S., *J. Med. Chem.* **2012,** *55* (3), 1137-1146.

4. Jo, H.; Meinhardt, N.; Wu, Y.; Kulkarni, S.; Hu, X.; Low, K. E.; Davies, P. L.; DeGrado, W. F.; Greenbaum, D. C., *J. Am. Chem. Soc.* **2012**, *134*, 17704-13.

5. Gupta, P. K.; Reid, R. C.; Liu, L.; Lucke, A. J.; Broomfield, S. A.; Andrews, M. R.; Sweet, M. J., Fairlie, D. P. *Bioorg. Med. Chem. Lett*. **2010**, *20*, 7067-70.

6. Dreier, L.; Wider, G. *Magn. Reson. Chem.* **2006**, *44,* S206-12.

7. Luo, P. Z.; Baldwin, R. L. *Biochemistry* **1997**, *36*, 8413-8421. Wallimann, P.; Kennedy, R. J.; Kemp, D. S. *Angew. Chem., Int. Ed.* **1999**, *38*, 1290-1292).

8. Brooks, B. R.; Bruccoleri, R. E.; Olafson, B. D.; States, D. J.; Swaminathan, S.; Karplus, M. *J. Comput. Chem.* **1983**, *4,* 187.

SUPPORTING FIGURES

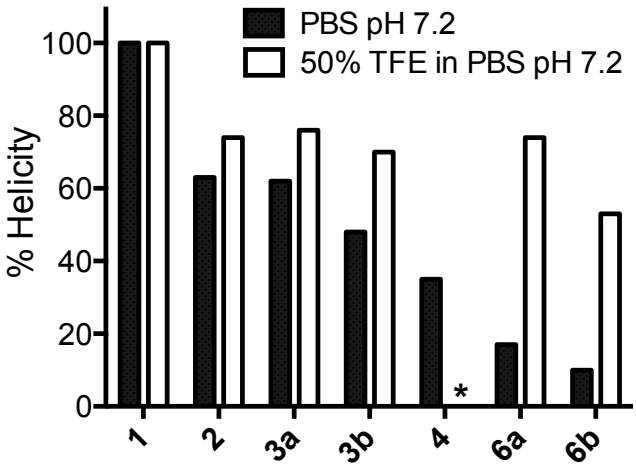

Figure S1. % Helicity based on molar elipticity at 215 nm at 298K in 10 mM phosphate buffer or in 50% TFE/10 mM PBS pH 7.2. * The CD fingerprint of *m*-xylene staple **4** in 50% TFE/10mM PBS pH 7.2 is of an unknown configuration and % helicity was not calculated. For the same reason, % helicity of peptide **5** in both conditions was not determined.

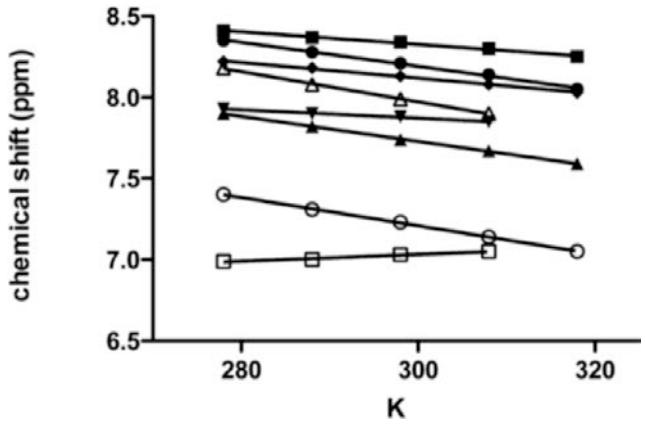

Figure S2. Temperature dependence of the amide NH chemical shifts for **1** in H_2O/D_2O (9:1). Line slopes indicating temperature coefficients ($\Delta\delta/T$) for each residue are shown in brackets. ● Lys 1 [7.4 ppb/K], ■ Ala 2 [3.9 ppb/K], ▲ Ala 3 [7.7 ppb/K], ▼ Ala 4 [2.6 ppb/K], ◆ Asp 5 [4.8 ppb/K], ○ Amide 1 [8.7 ppb/K], □ Amide 2 [2.1 ppb/K], △ side-chain lactam [9.3 ppb/K].

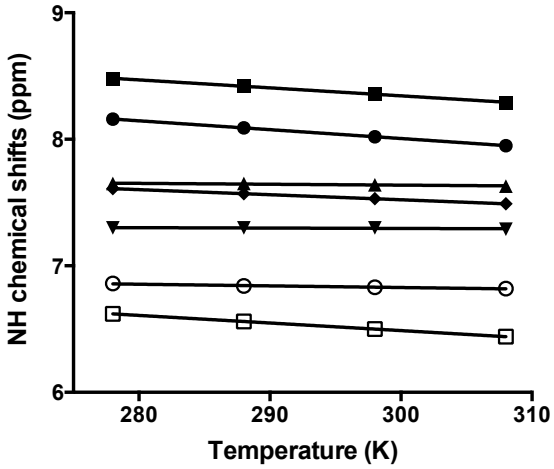

Figure S3. Temperature dependence of the amide NH chemical shifts for **2** in H_2O/ACN-d3 (1:1). Line slopes indicating temperature coefficients ($\Delta\delta/T$) for each residue are shown in brackets. ● X 1 [7.0 ppb/K], ■ Ala 2 [6.3 ppb/K], ▲ Ala 3 [0.7 ppb/K], ▼ Ala 4 [0.3 ppb/K], ◆ Asp 5 [4.0 ppb/K], ○ Amide 1 [1.3 ppb/K], □ Amide 2 [6.0 ppb/K].

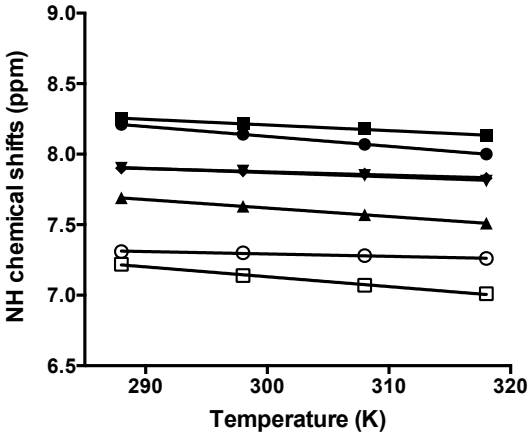

Figure S4. Temperature dependence of the amide NH chemical shifts for **3a** in H_2O/ACN-d3 (1:1). Line slopes indicating temperature coefficients ($\Delta\delta/T$) for each residue are shown in brackets. ● X 1 [7.0 ppb/K], ■ Ala 2 [4.0 ppb/K], ▲ Ala 3 [6.0 ppb/K], ▼ Ala 4 [3.0 ppb/K], ◆ Asp 5 [2.3 ppb/K], ○ Amide 1 [1.7 ppb/K], □ Amide 2 [7.0 ppb/K].

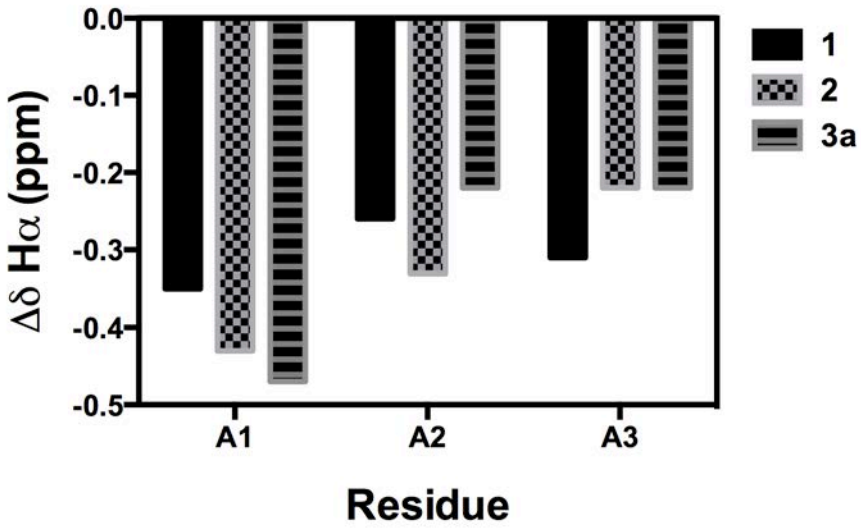

Fig. S5. Differences between observed chemical shift and random coil values ($\Delta\delta = \delta - \delta_{random*}$) for peptides **1, 2 and 3a in H_2O/D_2O (9:1). Negative values > -0.1ppm indicate upfield shifts that are typically observed for helical residues. This figure shows no clear differences between the three peptides in terms of alpha proton chemical shifts differences.**

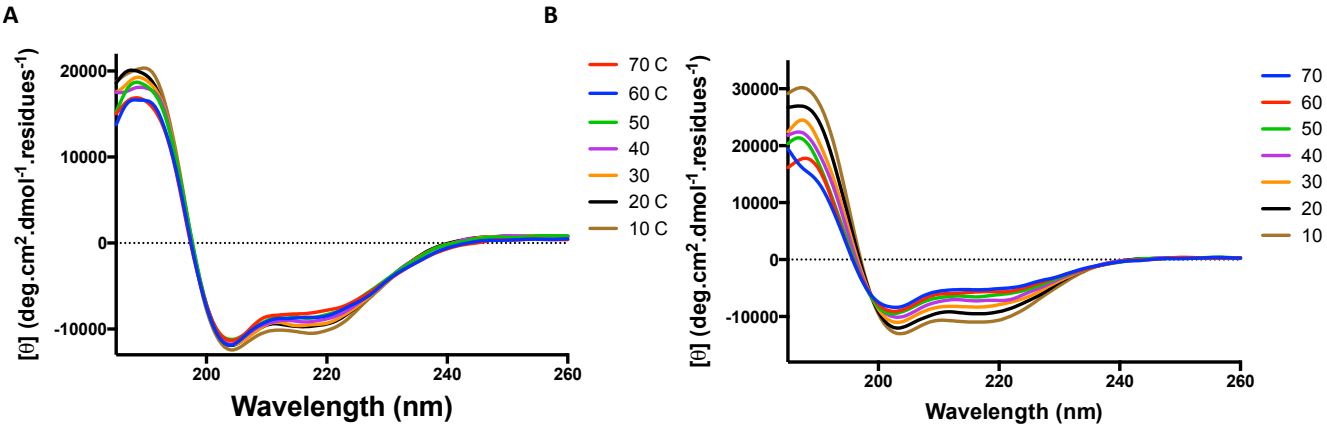

Figure S6. Variable temperature (^{0}C) circular dichroism spectra of (**A**) **2** and (**B**) **3a** in 10mM phosphate buffer (pH 7.4) showing temperature-induced unwinding of the helix. Similar pattern is also displayed by peptide **1** (data reported elsewhere).

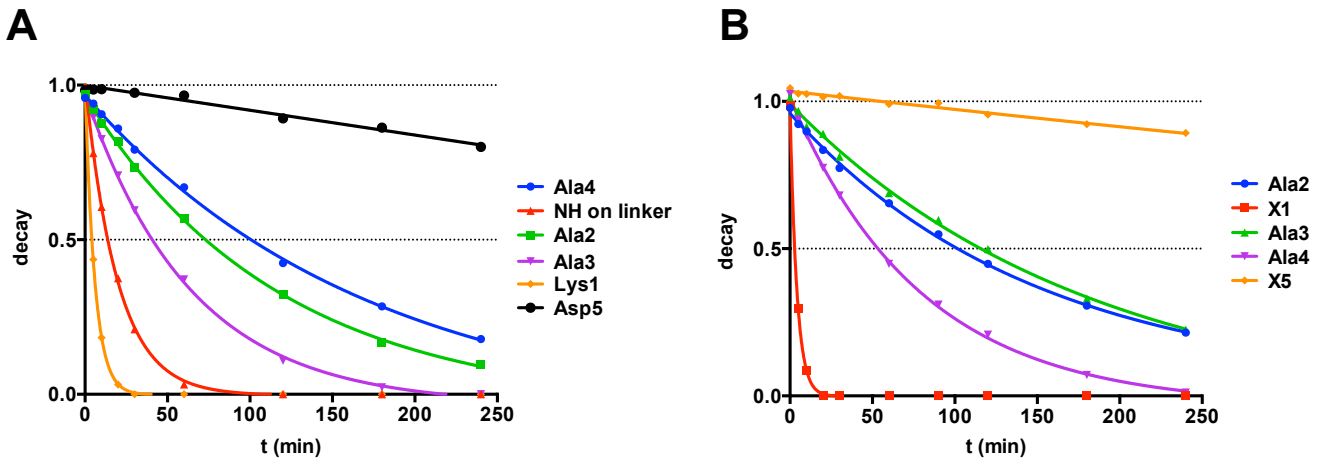

Figure S7. H-D exchange rate of the amides NHs for **1** (**A**) and **2** (**B**) in DMSO-d_6 at 298 K. The fast NH exchange rate is similar for the two compounds.

ANALYTICAL DATA (HPLC)

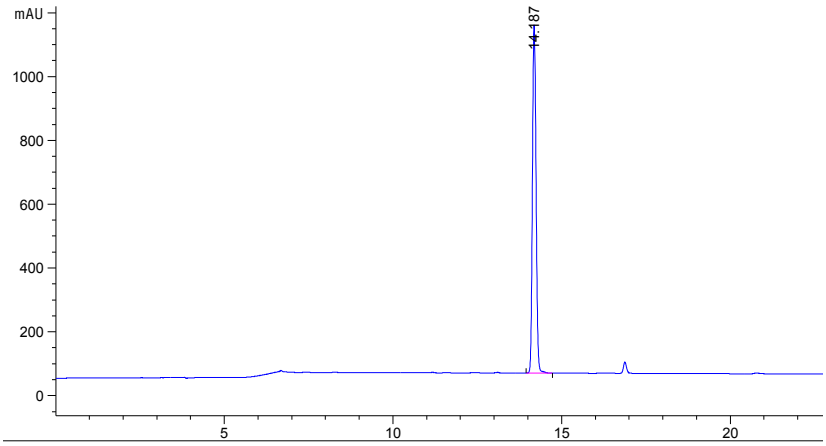

Figure S8. HPLC chromatogram of the pure cyclopentapeptide **1a**.

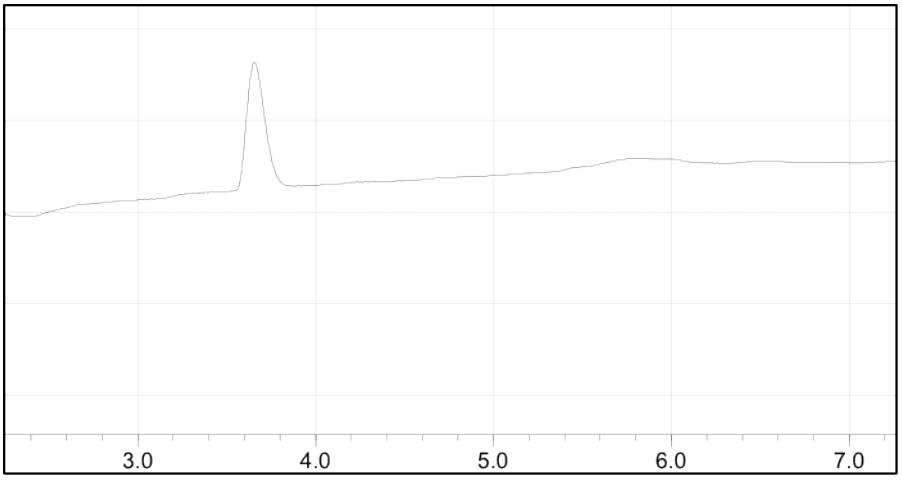

Figure S9. HPLC chromatogram of the pure cyclopentapeptide **1b**.

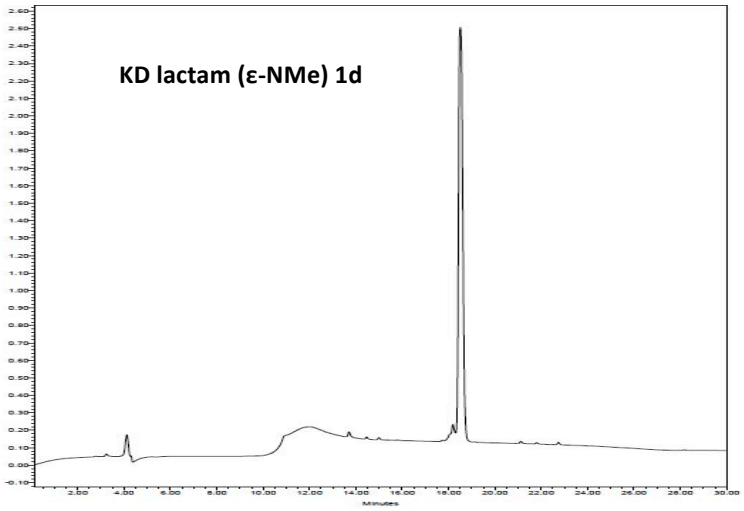

Figure S10. HPLC chromatogram of the pure cyclopentapeptide **1c**.

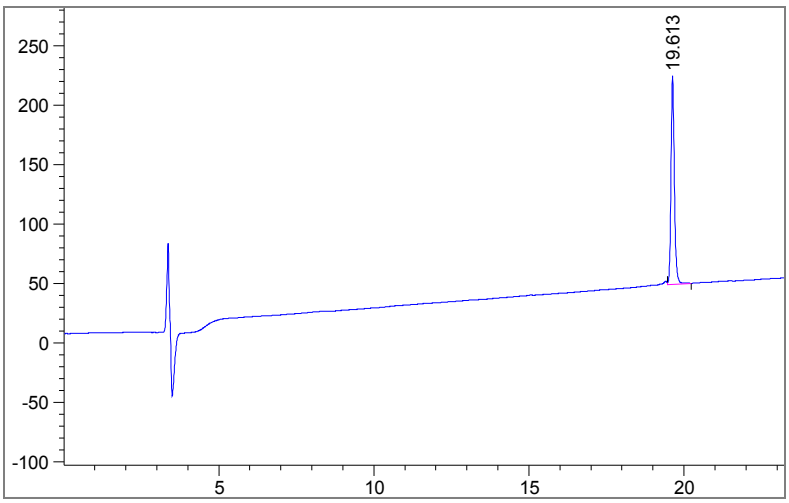

Figure S11. HPLC chromatogram of the pure cyclopentapeptide **2**.

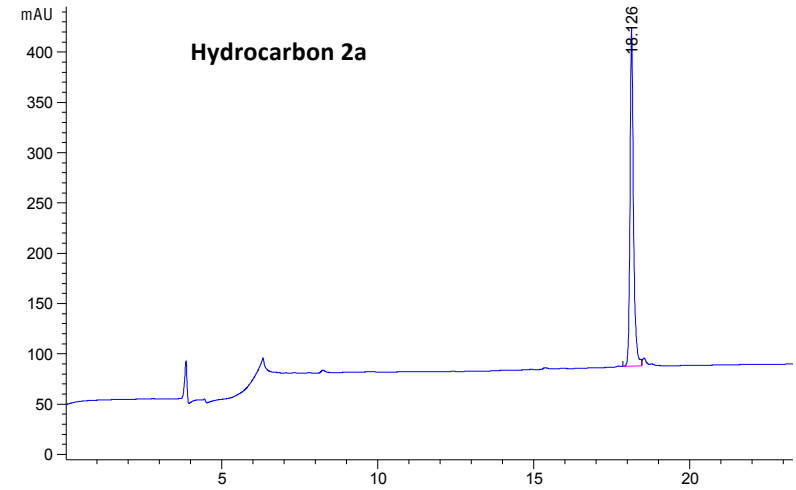

Figure S12. HPLC chromatogram of the pure cyclopentapeptide **2a**.

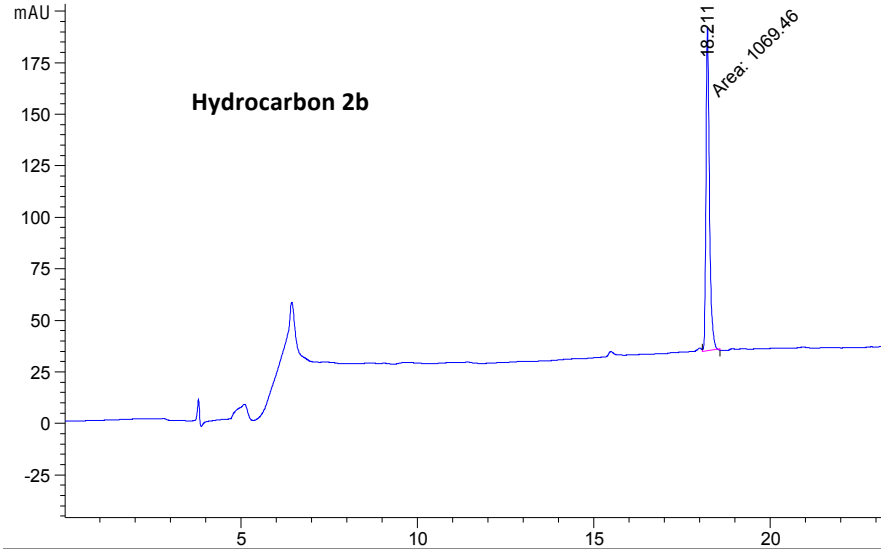

Figure S13. HPLC chromatogram of the pure cyclopentapeptide **2b**.

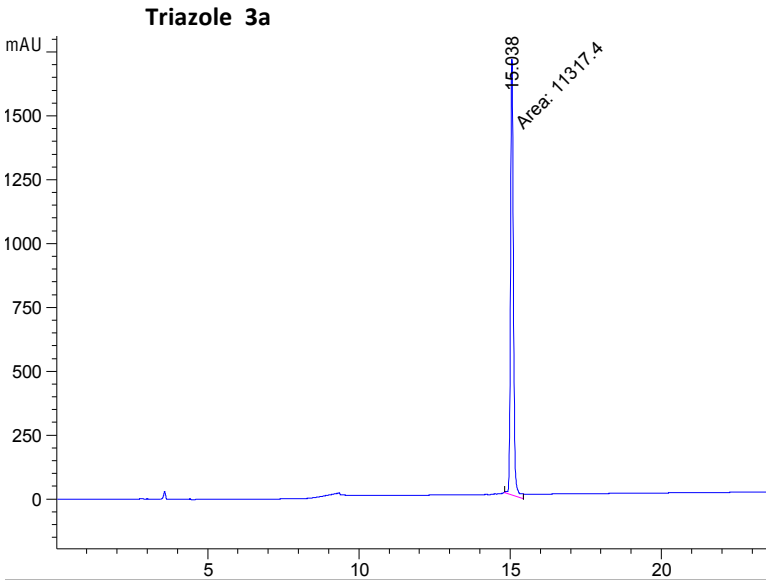

Figure S14. HPLC chromatogram of the pure cyclopentapeptide **3a**.

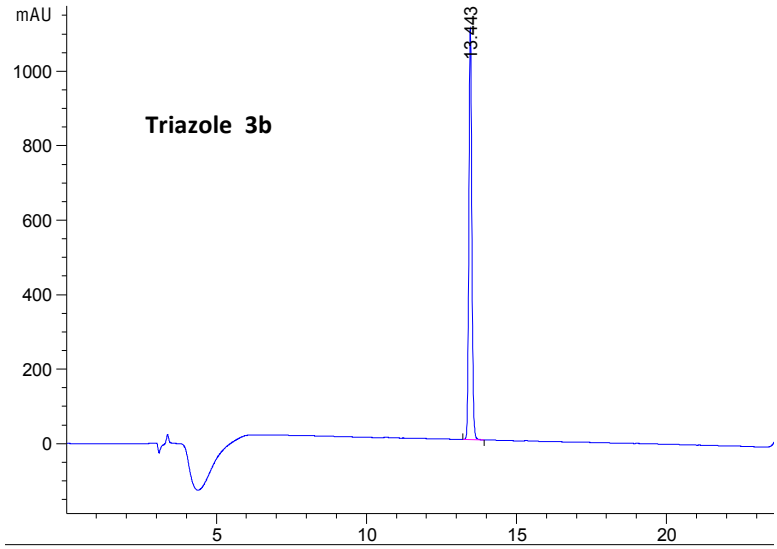

Figure S15. HPLC chromatogram of the pure cyclopentapeptide **3b**.

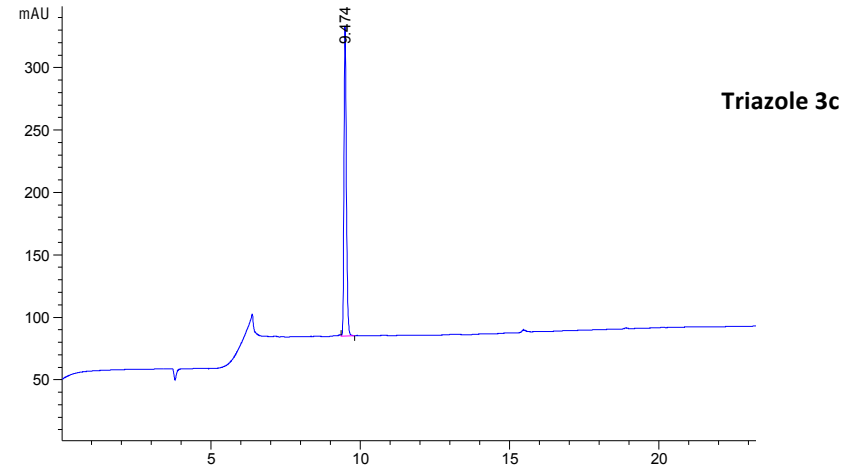

Figure S16. HPLC chromatogram of the pure cyclopentapeptide **3c**.

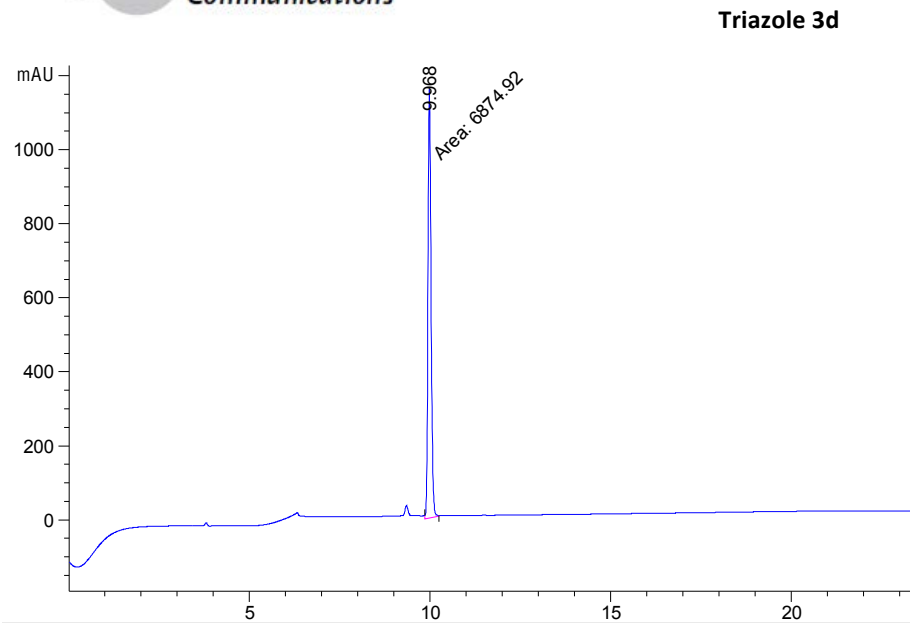

Figure S17. HPLC chromatogram of the pure cyclopentapeptide **3d**

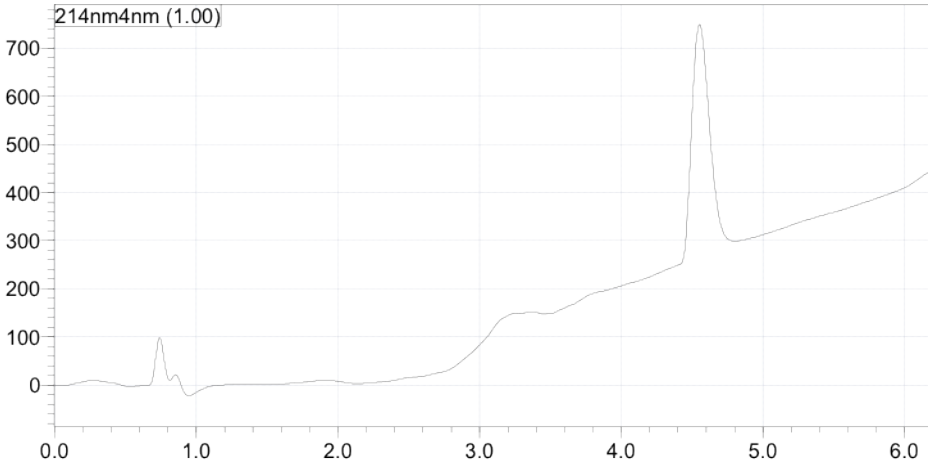

Figure S18. UHPLC chromatogram of the pure cyclopentapeptide **4.**

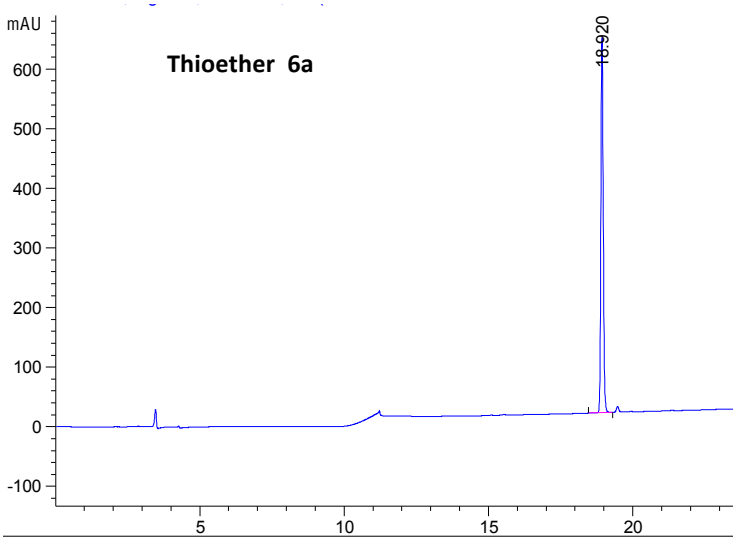

Figure S19. HPLC chromatogram of the pure cyclopentapeptide **6a**.

Thioether **6b**

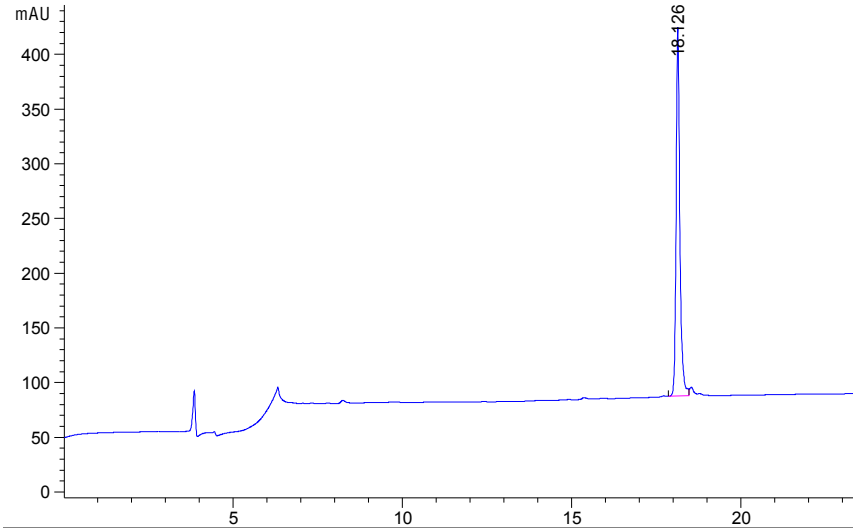

Figure S20. HPLC chromatogram of the pure cyclopentapeptide **6b**.

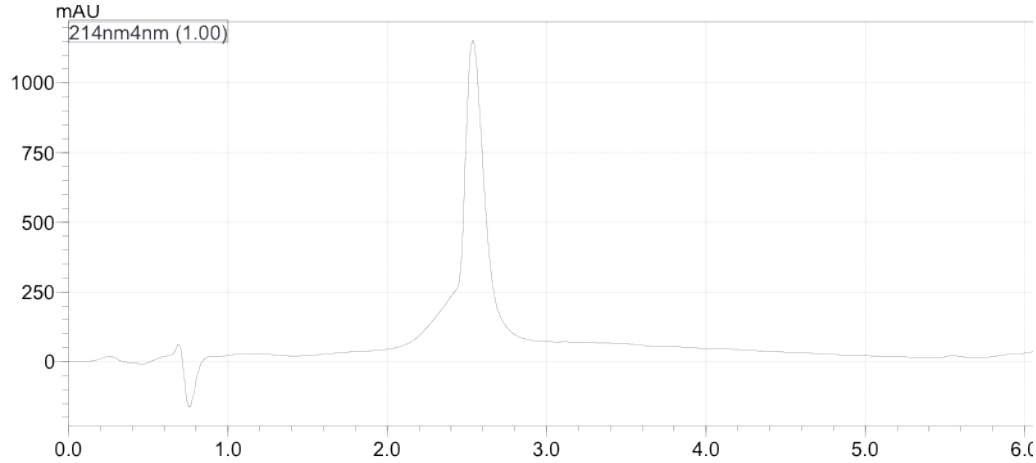

Figure S21. UHPLC chromatogram of the pure 18mer **9**.

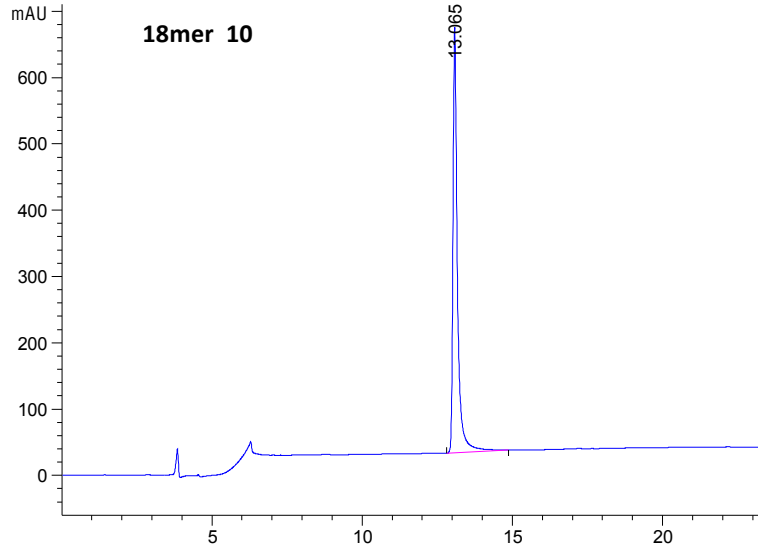

Figure S22. HPLC chromatogram of the pure 18mer **10**.

ANALYTICAL DATA (NMR-1D)

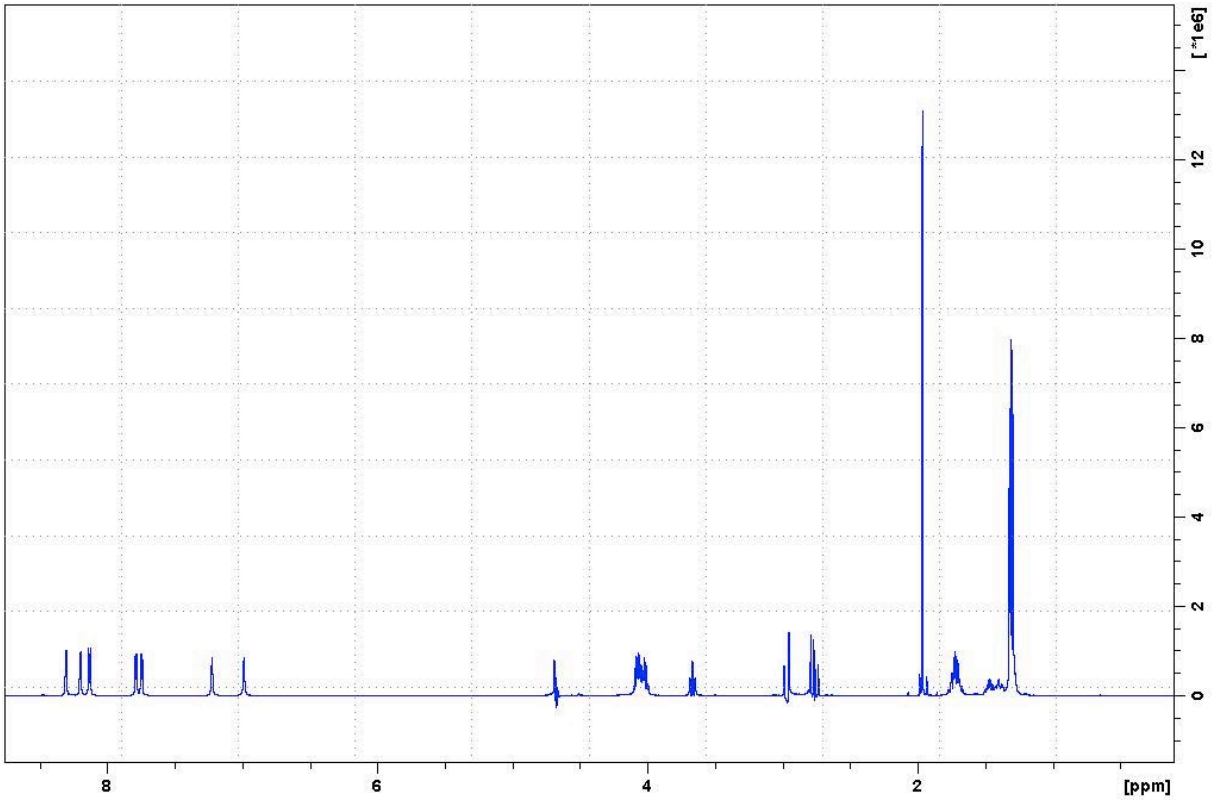

Figure S23. 600MHz ^{1}H NMR spectrum of **1a** in H_2O/D_2O (9:1) at 298K.

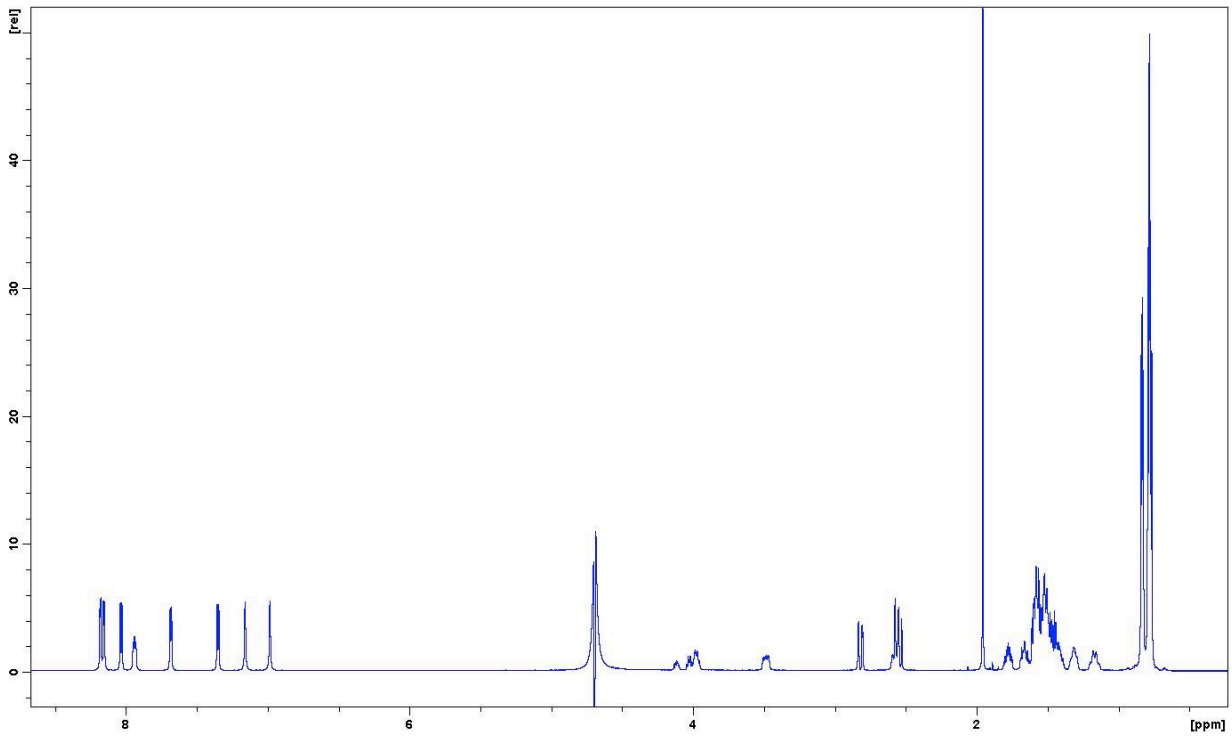

Figure S24. 600MHz ^{1}H NMR spectrum of **1b** in H_2O/D_2O (9:1) at 298K.

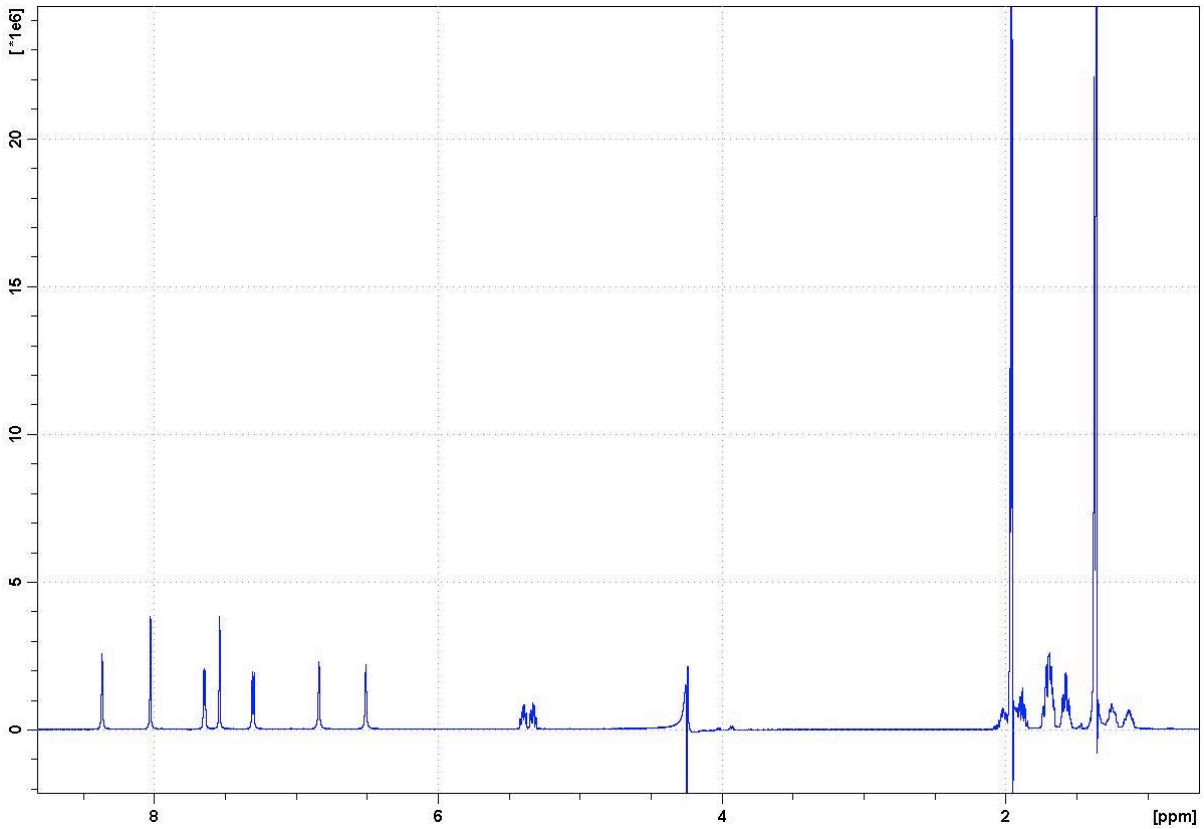

Figure S25. 600MHz ^{1}H NMR spectrum of **2** in H_2O/CD3CN (1:1) at 298K.

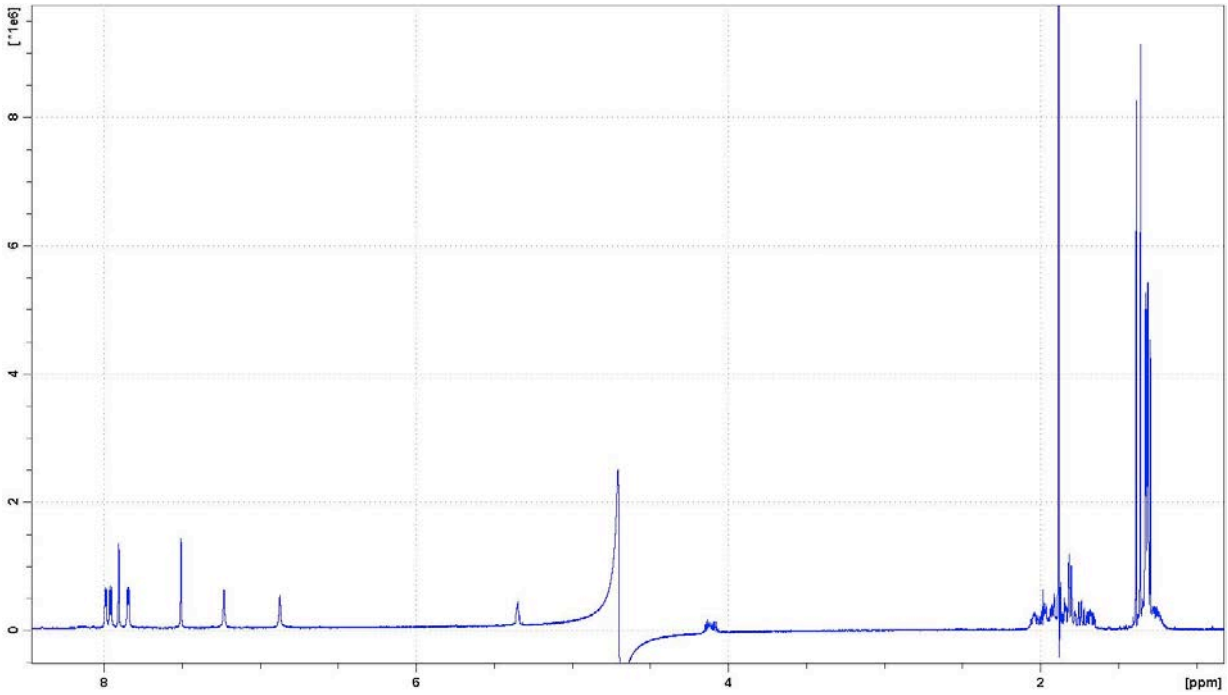

Figure S26. 600MHz ^{1}H NMR spectrum of **2a** in H_2O/D_2O (9:1) at 298K.

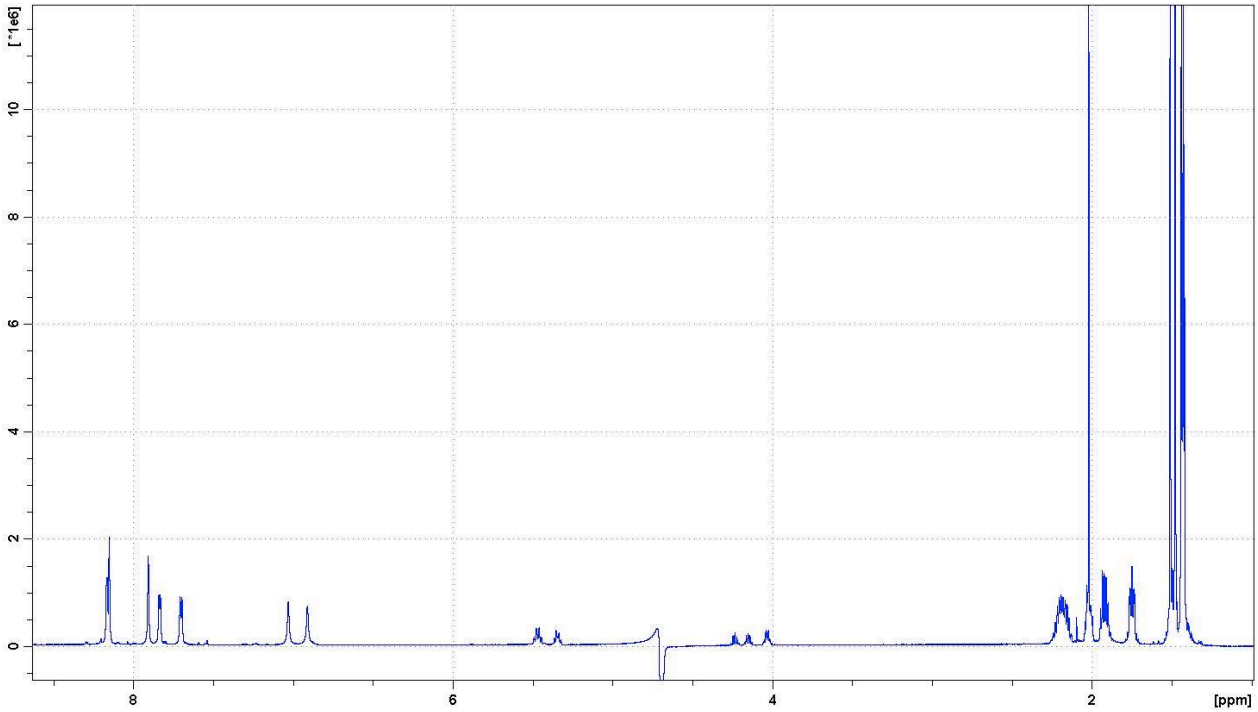

Figure S27. 600MHz ^{1}H NMR spectrum of **2b** in H_2O/D_2O (9:1) at 298K.

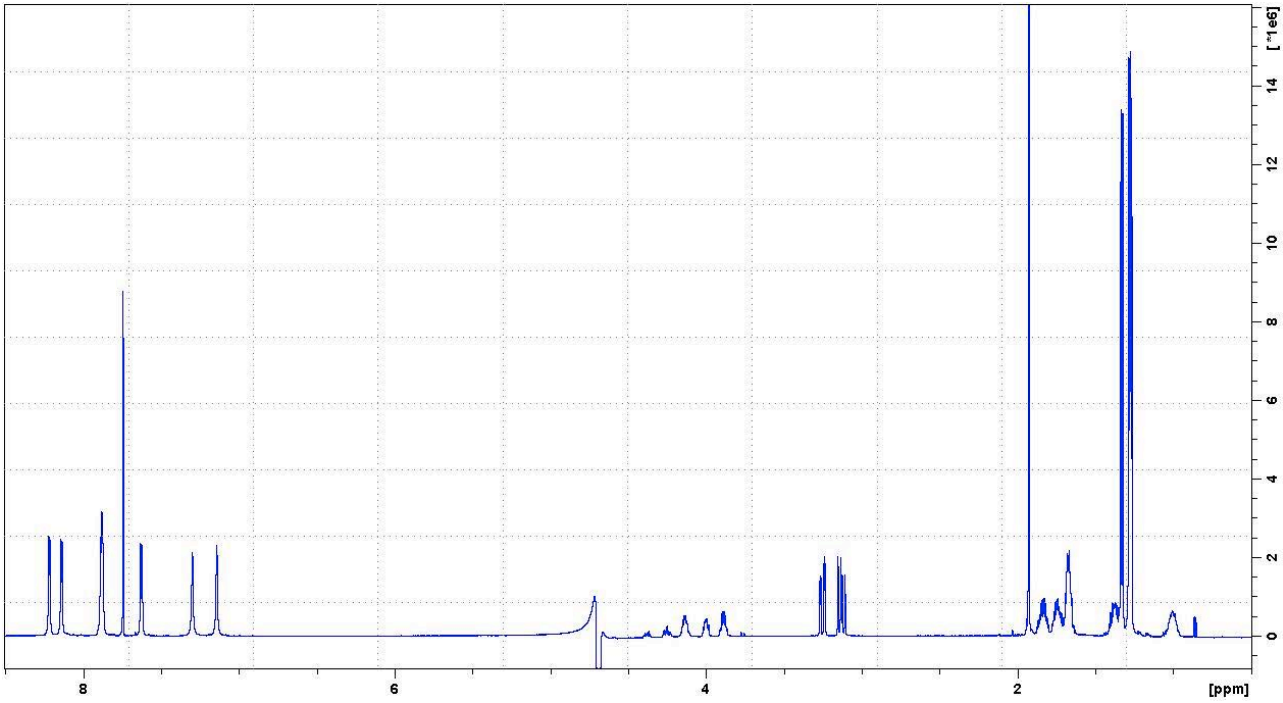

Figure S28. 600MHz ^{1}H NMR spectrum of **3a** in H_2O/CD3CN (1:1) at 298K.

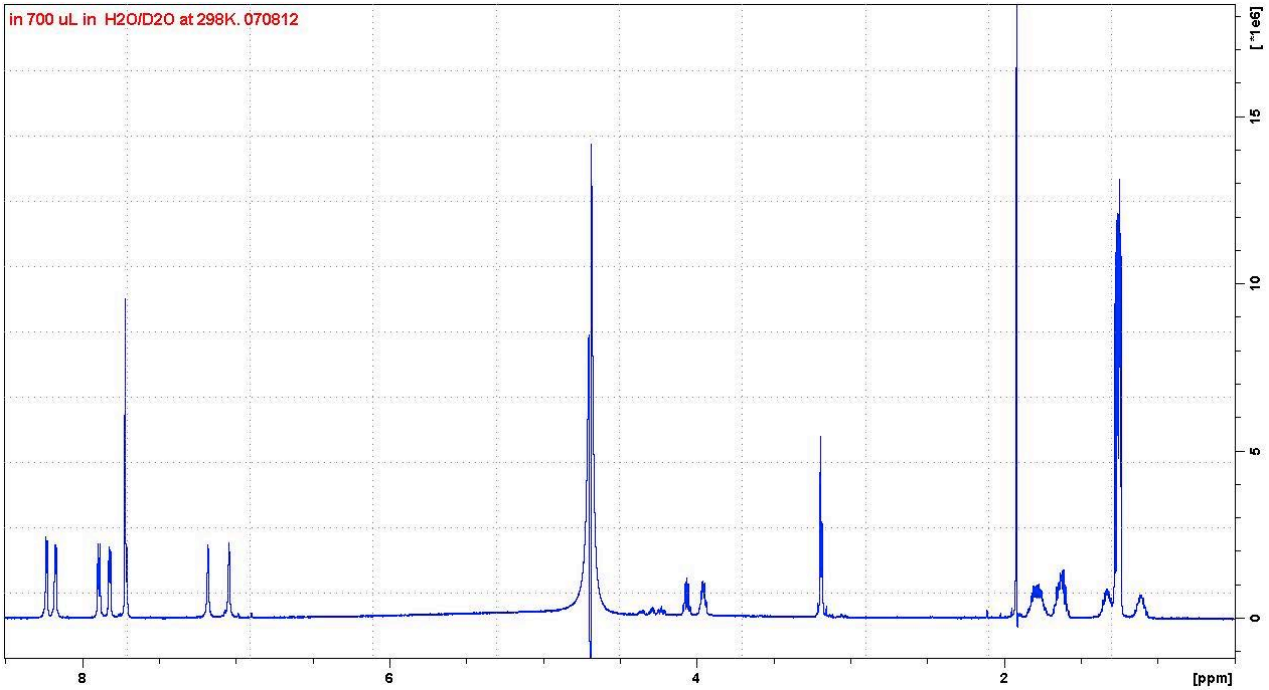

Figure S29. 600MHz ^{1}H NMR spectrum of **3b** in H_2O/D_2O (9:1) at 298K.

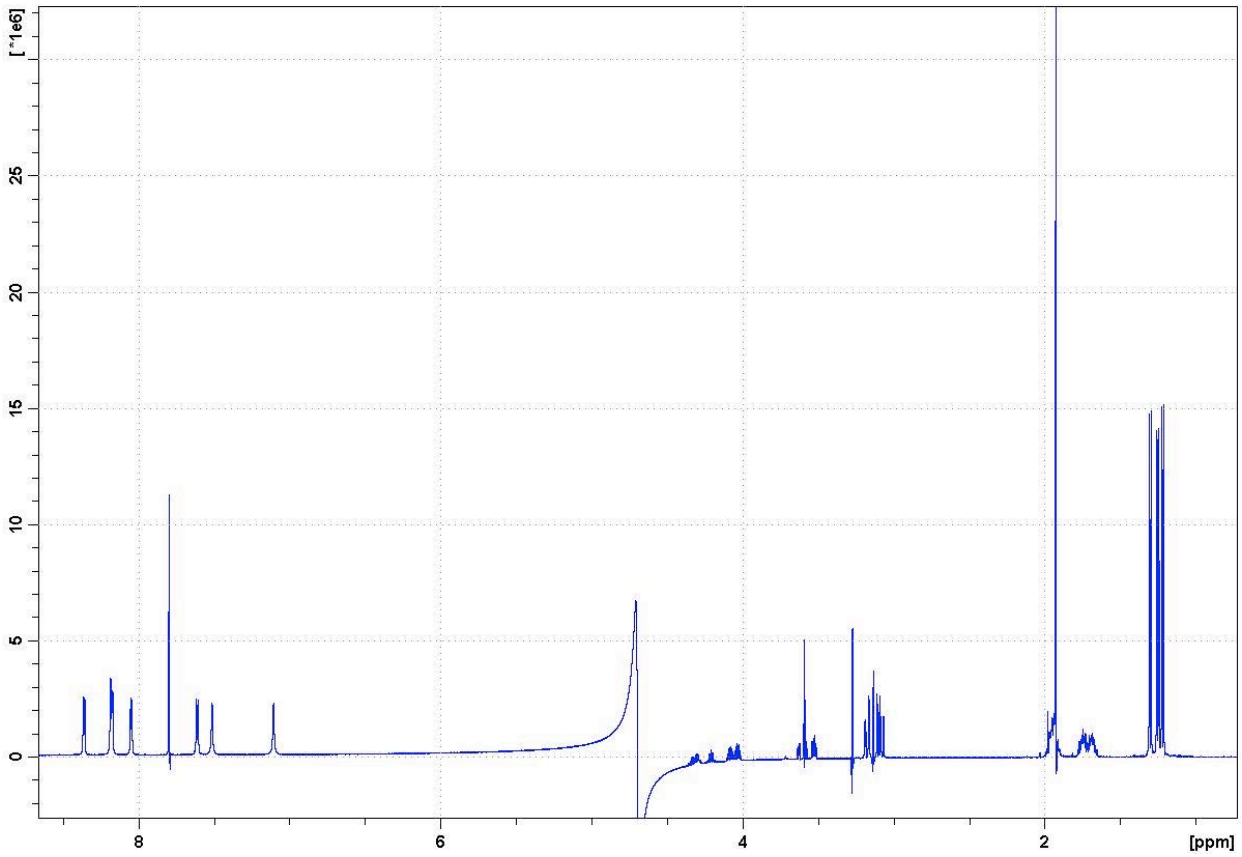

Figure S30. 600MHz ^{1}H NMR spectrum of **3c** in H_2O/D_2O (9:1) at 298K.

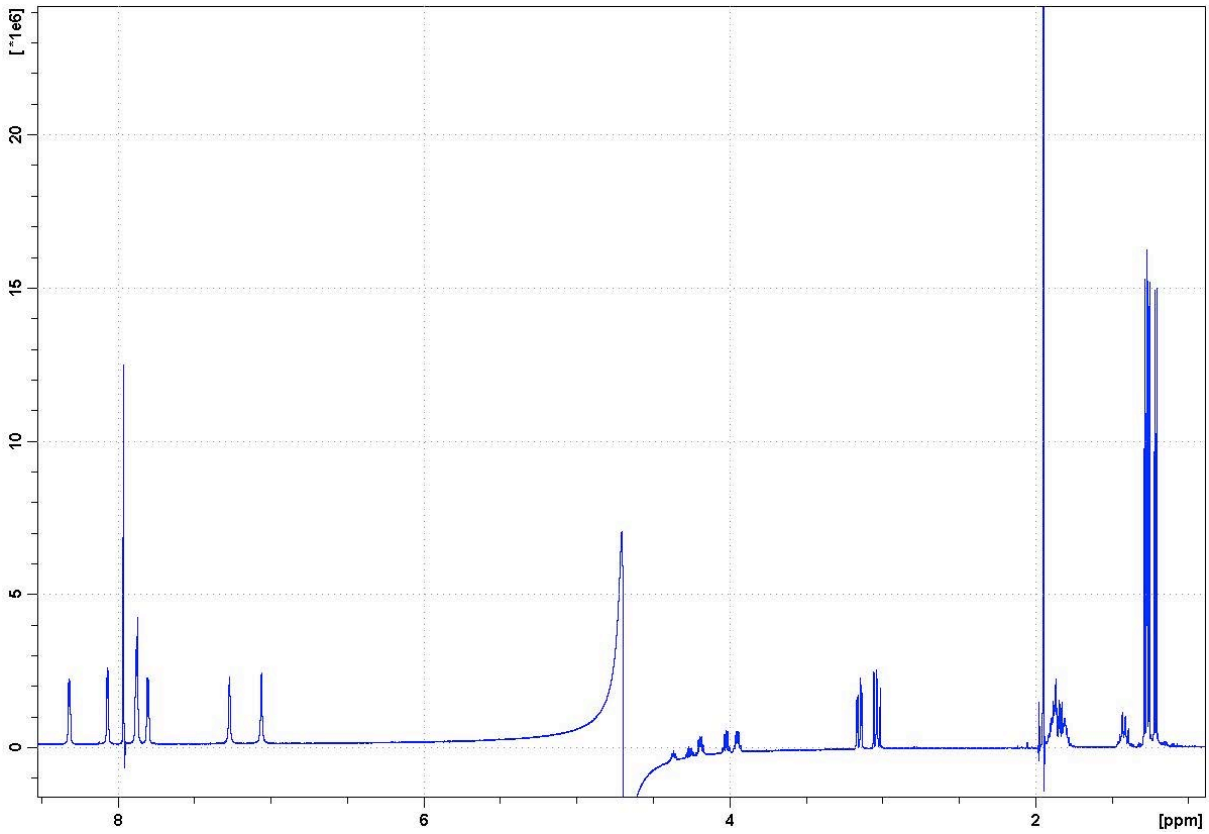

Figure S31. 600MHz ^{1}H NMR spectrum of **3d** in H_2O/D_2O (9:1) at 298K.

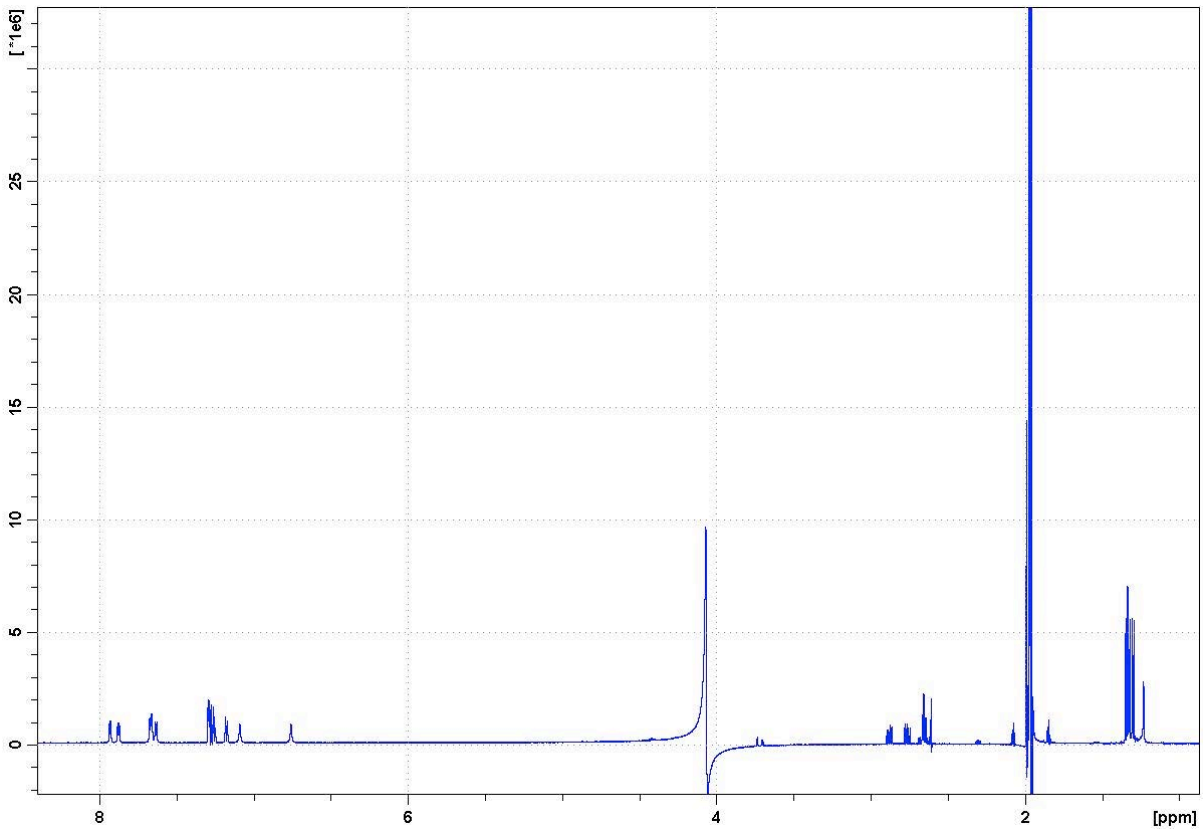

Figure S32. 600MHz ^{1}H NMR spectrum of **4** in H_2O/D_2O (9:1) at 298K.

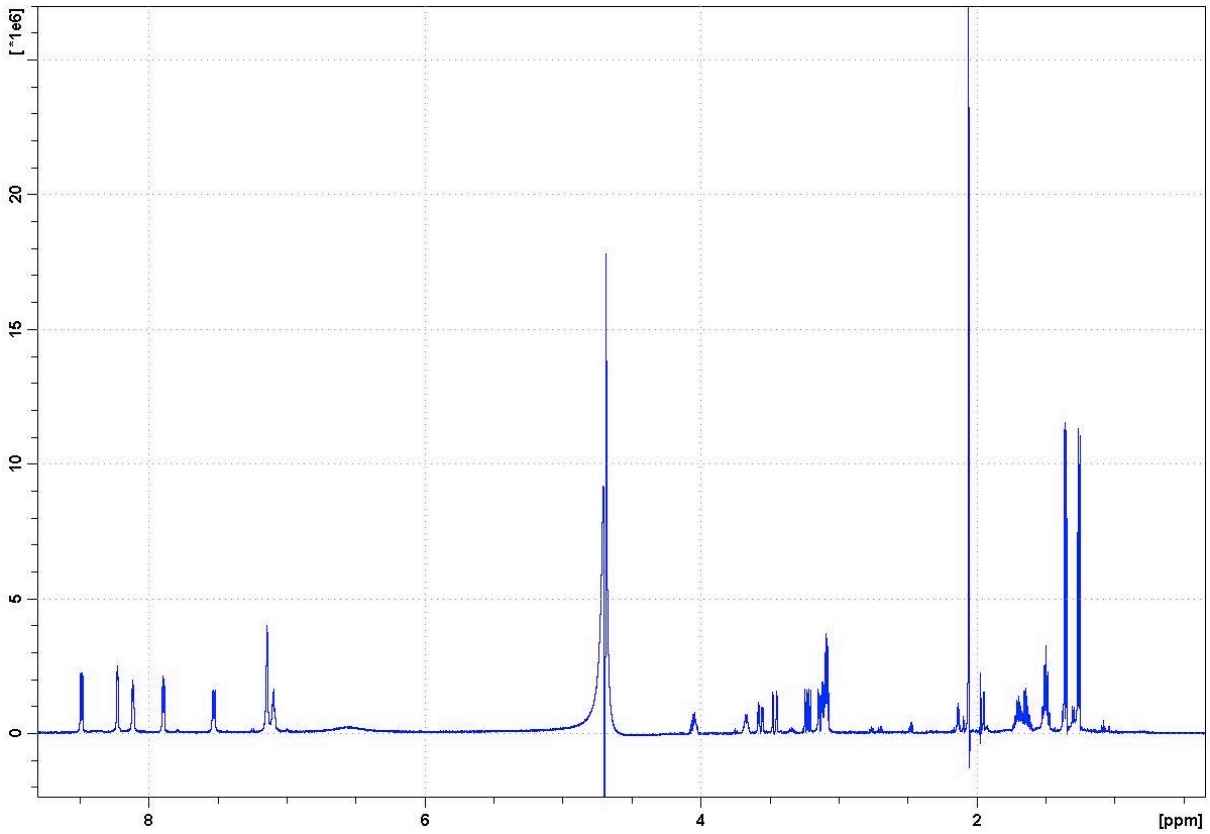

Figure S33. 600MHz ^{1}H NMR spectrum of **5** in H_2O/D_2O (9:1) at 298K.

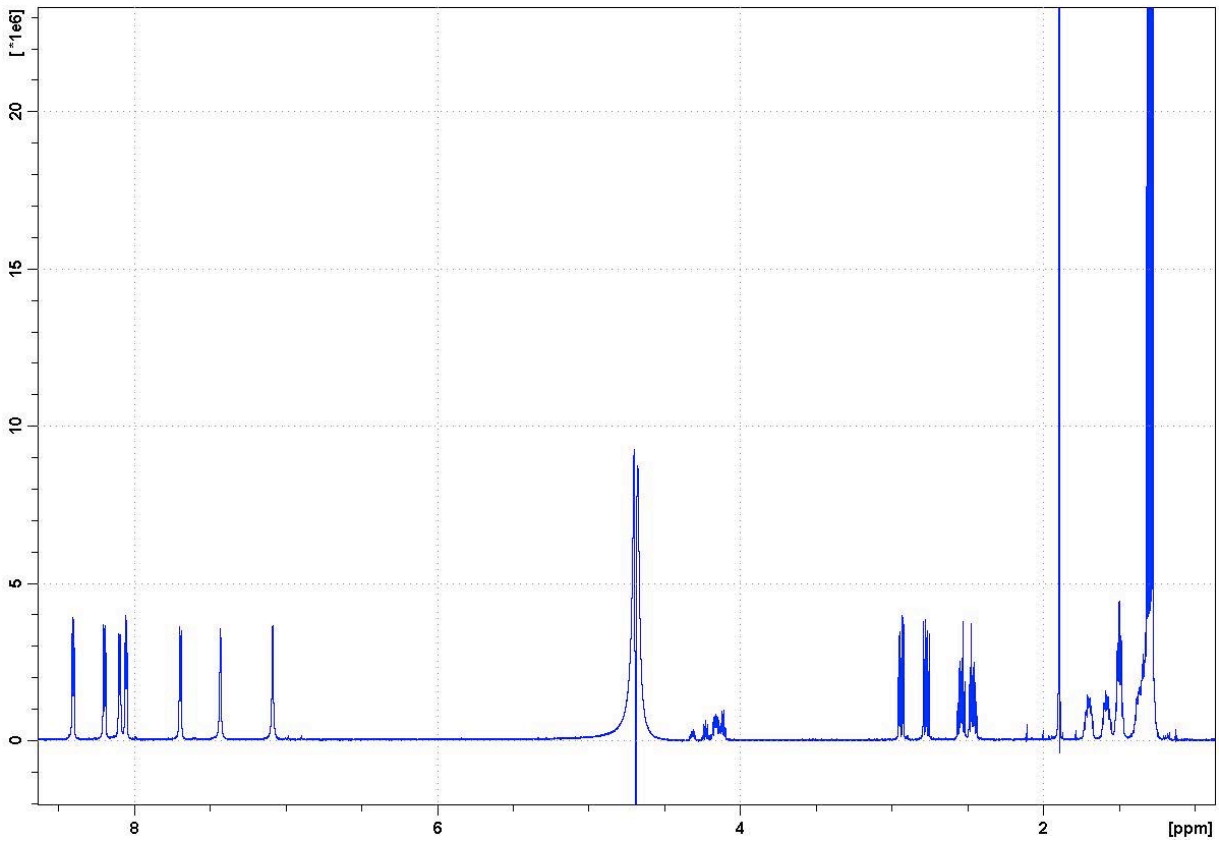

Figure S34. 600MHz ^{1}H NMR spectrum of **6a** in H_2O/D_2O (9:1) at 298K.

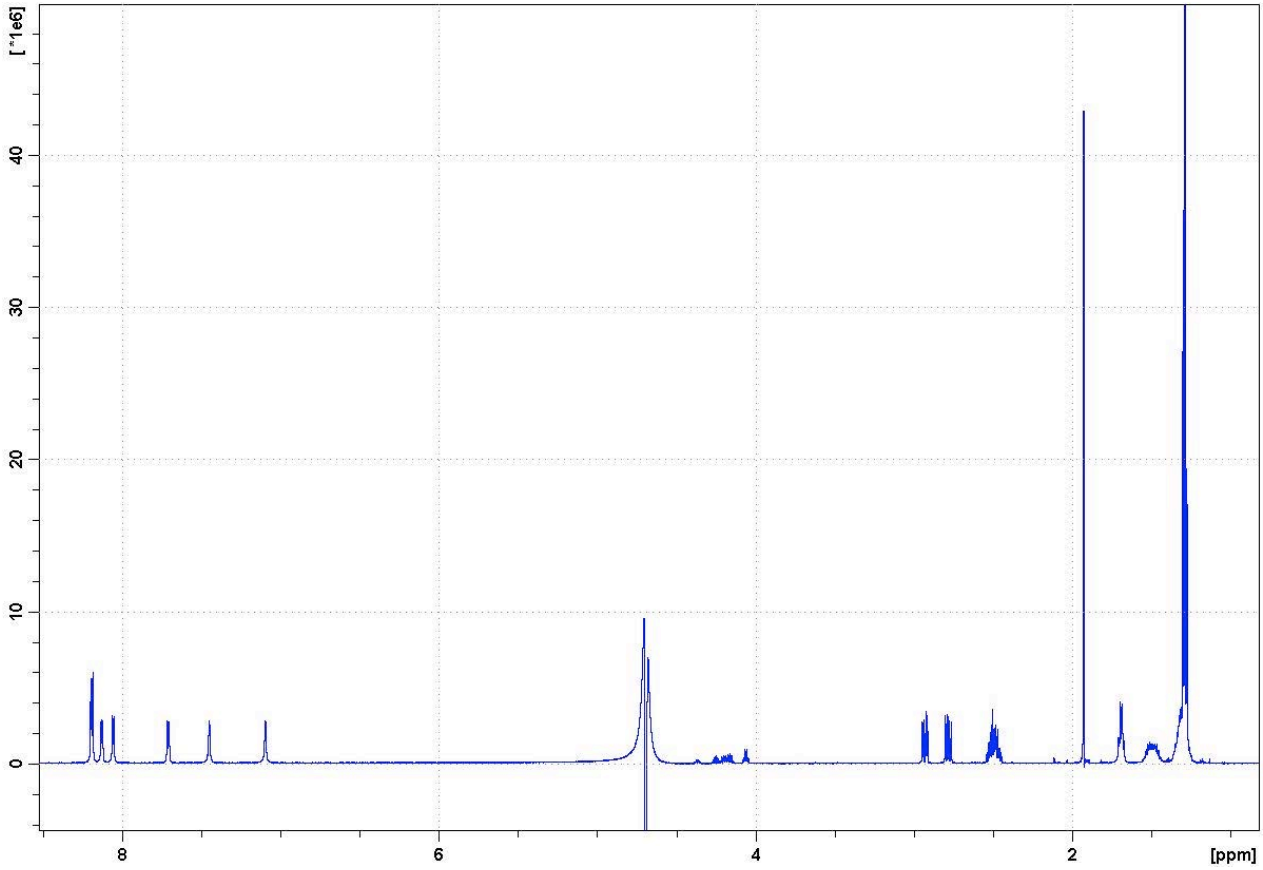

Figure S35. 600MHz ^{1}H NMR spectrum of **6b** in H_2O/D_2O (9:1) at 298K.

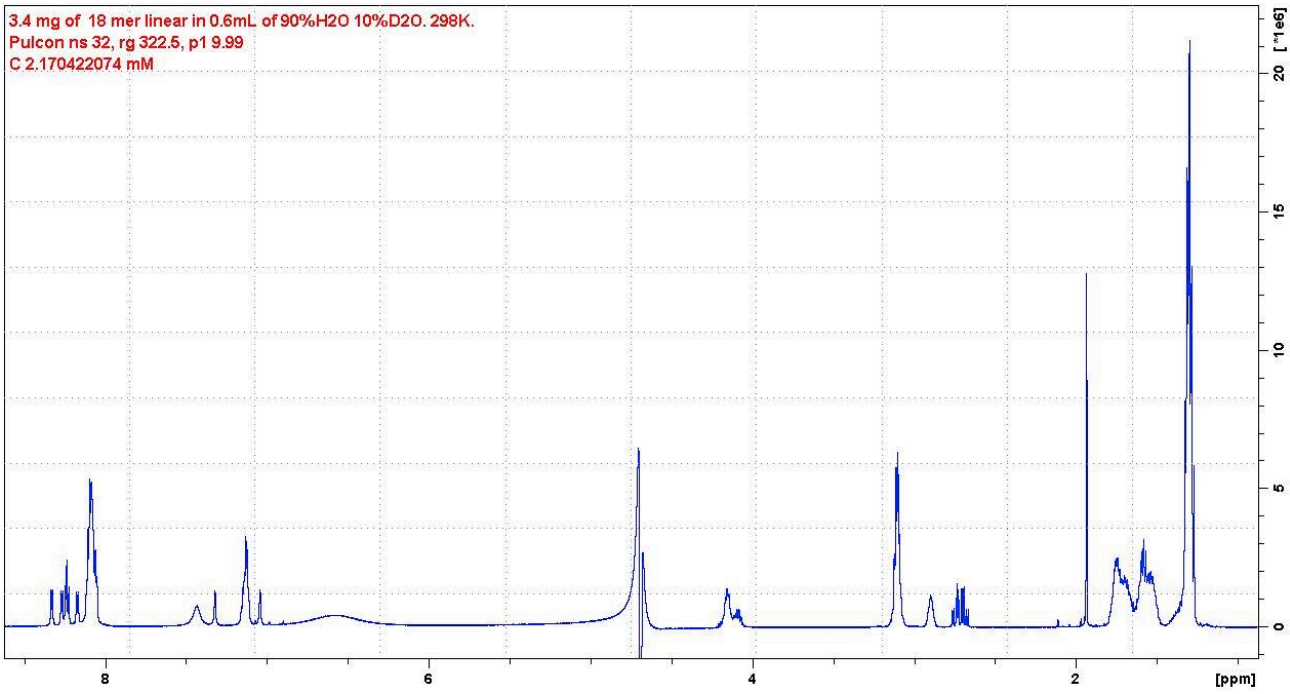

Figure S36. 600MHz ^{1}H NMR spectrum of **7** in H_2O/D_2O (9:1) at 298K.

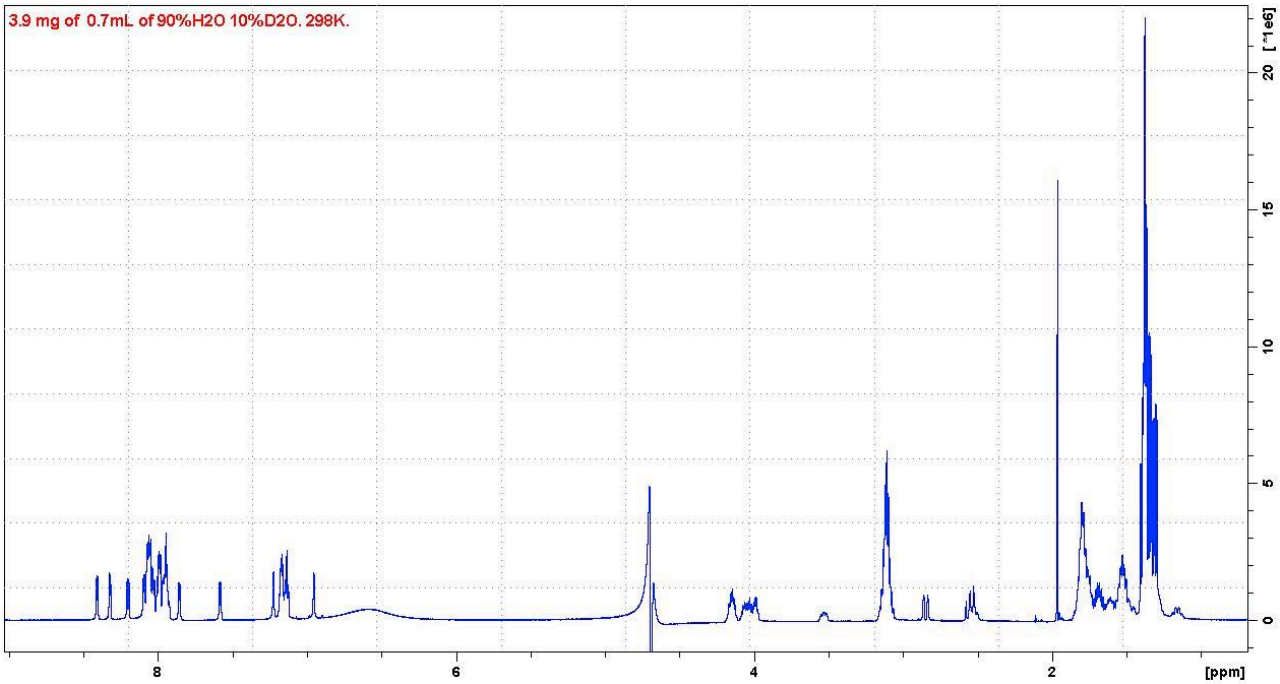

Figure S37. 600MHz ^{1}H NMR spectrum of **8** in H_2O/D_2O (9:1) at 298K.

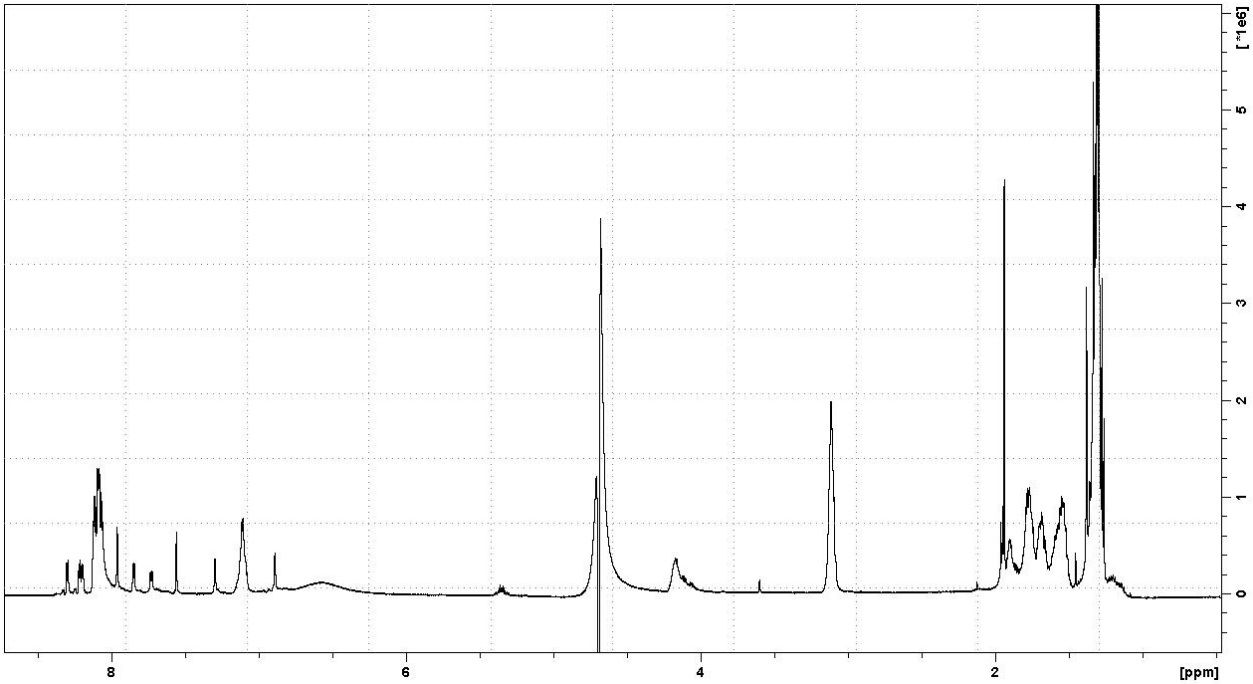

Figure S38. 600MHz ^{1}H NMR spectrum of **9** in H_2O/D_2O (9:1) at 298K.

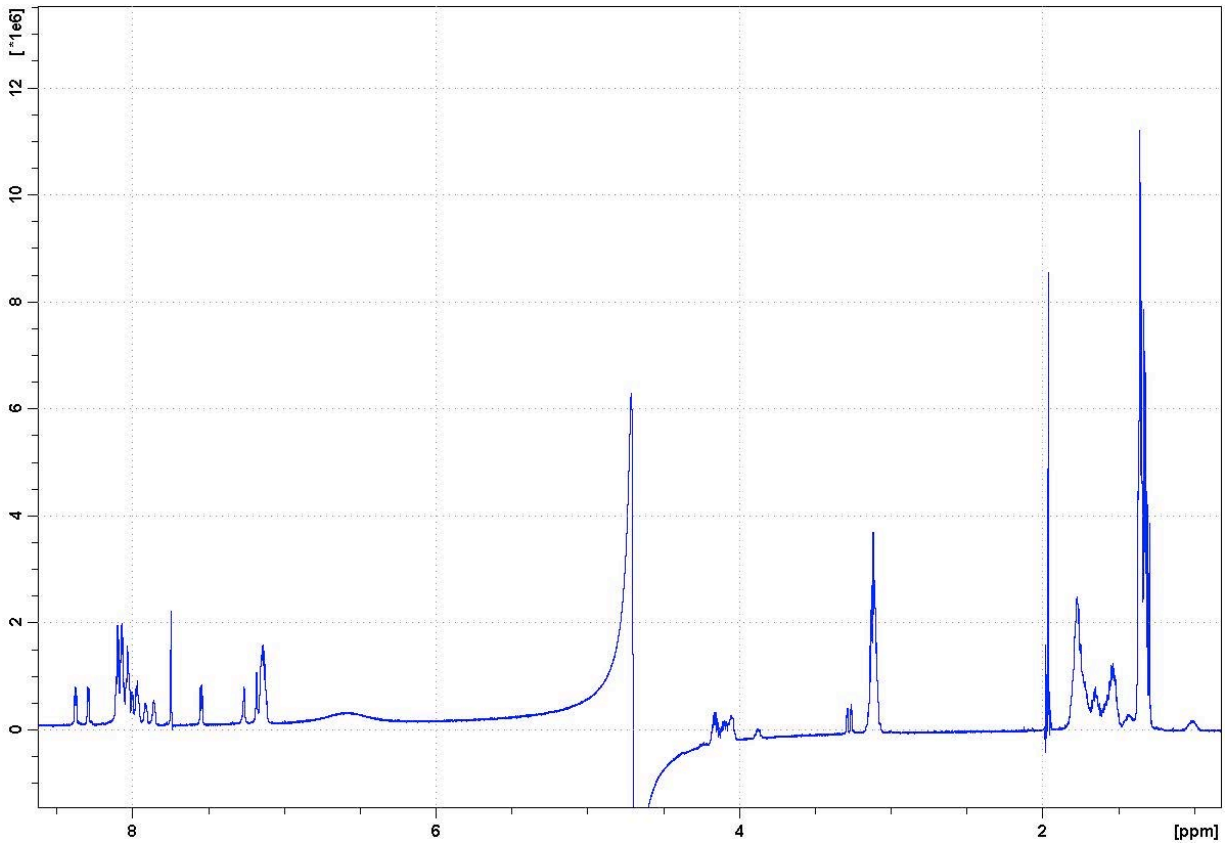

Figure S39. 600MHz ^{1}H NMR spectrum of **10** in H_2O/D_2O (9:1) at 298K.

Analytical Data (NMR-2D)

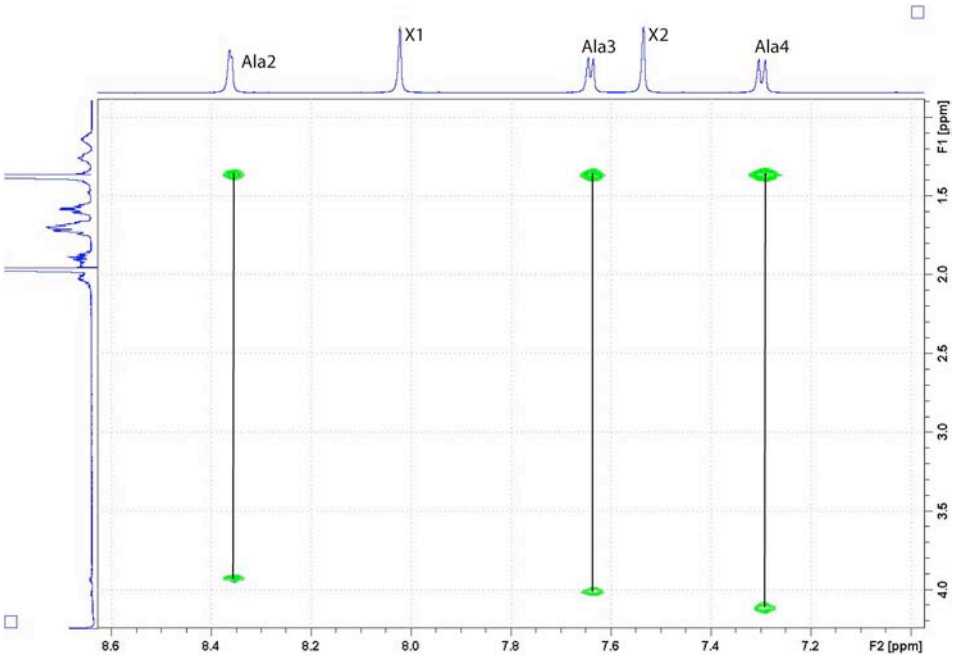

Figure S40. 600MHz TOCSY fingerprint region of **2** in H_2O/CD_3CN (1:1) at 298K. Connectivity of the NH, Cα, Cβ protons for the peptide is shown by the solid line.

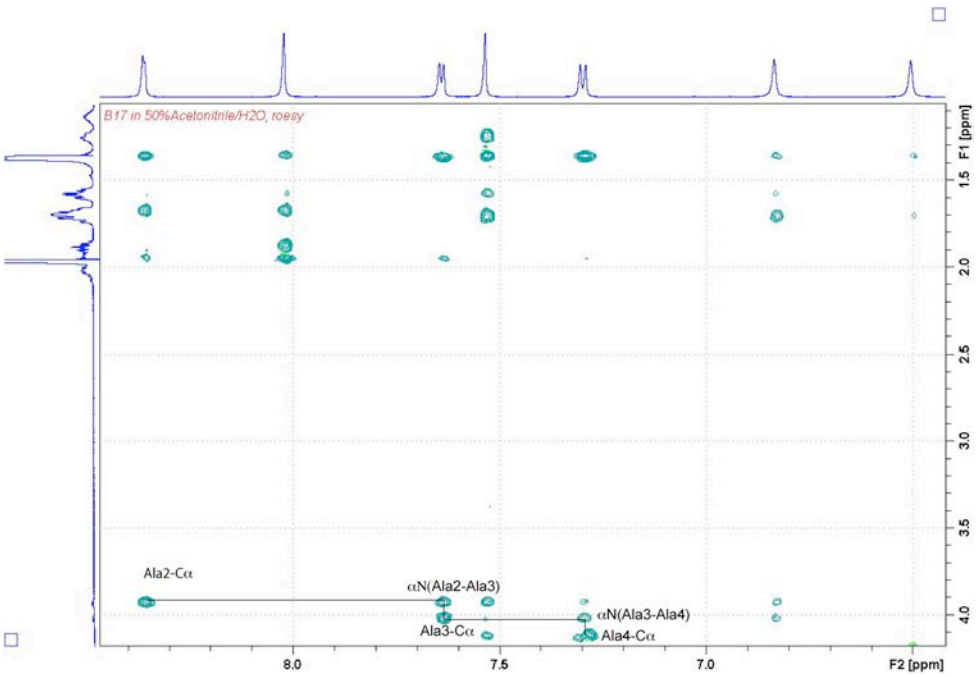

Figure S41. Magnified NH-CHα region from the 600MHz ROESY spectrum of **2** in H_2O/CD_3CN (1:1) at 298K. Sequential connectivity for the peptide is shown by the solid line.

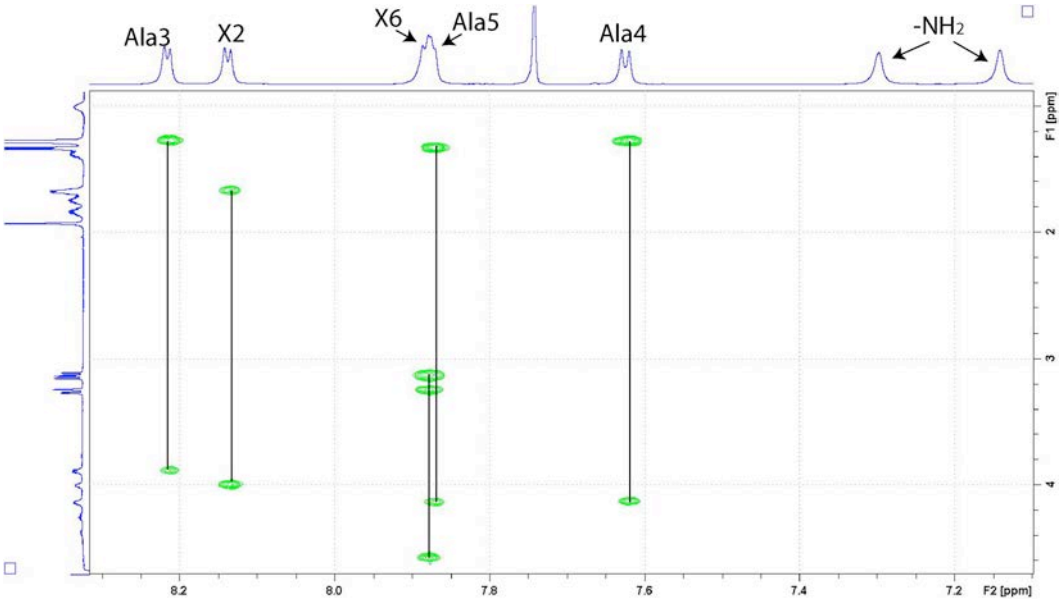

Figure S42. 600MHz TOCSY fingerprint region of **3a** in H_2O/D_2O (9:1) at 298K. Connectivity of the NH, Cα, Cβ protons for the peptide is shown by the solid line.

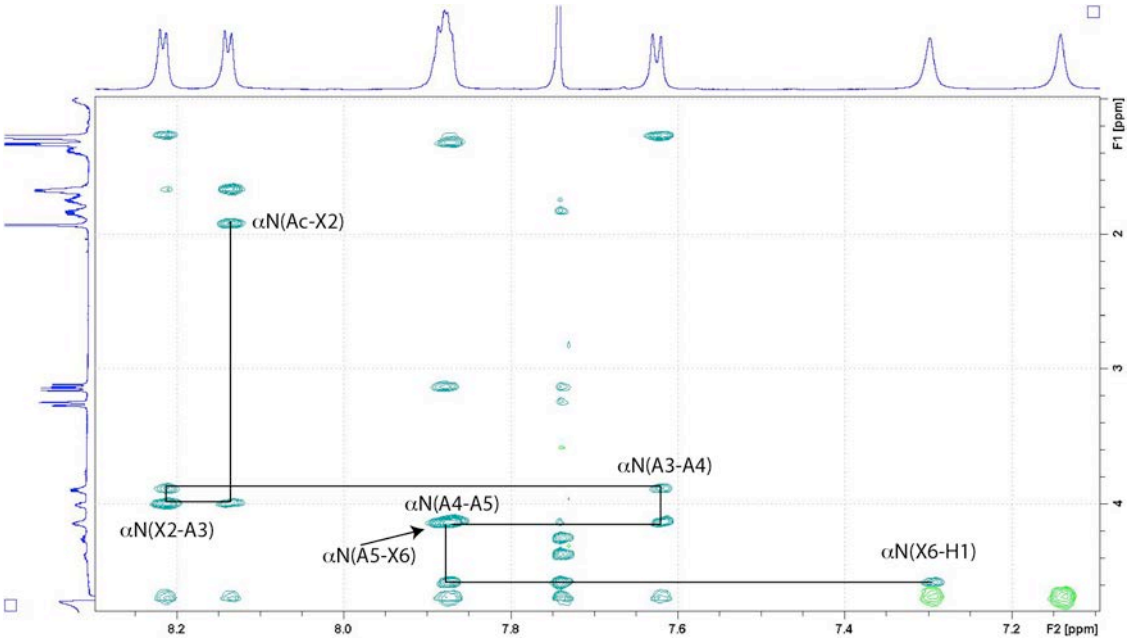

Figure S43. Magnified NH-CHα region from the 600MHz ROESY spectrum of **3a** in H_2O/D_2O (9:1) at 298K. Sequential connectivity for the peptide is shown by the solid line.

SUPPORTING TABLES

Table S1. Amide coupling constants ($^3J_{NHCH}\alpha$) and temperature coefficients for peptides KD lactam **1**, hydrocarbon **2** and triazole **3a**.

Residue	$^3J_{NHCH}\alpha$ (Hz)			Δδ/T (ppb/K)		
	1	**2**	**3a**	**1**	**2**	**3a**
X_1	3.6	*	4.7	7.4	7.0	6.8
A_2	3.7	2.8	4.4	3.9	6.5	4.0
A_3	5.2	6.1	5.8	7.7	0.6	5.8
A_4	4.6	7.7	5.3	2.6	0.6	2.9
X_5	7.0	*	6.8	4.8	4.0	2.2
NH_2T	*	*		2.1/8.7	1.3/6.0	1.5/7.0
NH lactam	7.8			9.3		

* singlet peaks

Table S2. ^{1}H NMR resonance assignments and chemical shifts (δ ppm) for **2** in H_2O/ACN (1:1) at 298K.

Residue	δ (ppm)			
	NH	**Hα**	**Hβ**	**Other**
Ac-S 2	8.02	n/a	1.57, 1.24	γCH_2 1.69, 1.36; δCH_2 2.01, 1.69; εCH_1 5.40; Acetyl Cα 1.96
Ala 3	8.36	3.92	1.36	
Ala 4	7.64	4.02	1.35	
Ala 5	7.30	4.13	1.36	
S 6 –NH_2	7.53	n/a	1.35, 1.13	γCH_2 1.69, 1.57; δCH_2 1.89, 1.57; εCH_1 5.32; NH1 6.83; NH2 6.50

Table S3. ROE-derived distances, $^3J_{NH\text{-}CH\alpha}$ derived j-angle restraints and hydrogen-bond restraints used for calculating the solution structure of **2** in H_2O/ACN (1:1) at 298K.

Acetyl1 Hα*	S2 HN	4.2 Å; Strong+ 1.5Å correction
Acetyl1 Hα*	Ala3 HN	6.0 Å; Very Weak, no correction
Acetyl1 Hα*	Ala4 HN	6.0 Å; Very Weak, no correction
Acetyl1 Hα*	Ala5 HN	6.0 Å; Very Weak, no correction
S2 HN	Ala3 HN	5.0 Å; Weak
Ala3 Hα	Ala4 HN	5.0 Å; Weak
Ala3 Hα	Ala5 HN	6.0 Å; Very Weak
Ala3 Hα	Ala6 HN	5.0 Å; Weak
Ala3 Hα	S6 H1	6.0 Å; Very Weak
Ala3 Hα	S6 H2	6.0 Å; Very Weak
Ala3 HN	Ala4 HN	3.5 Å; Medium
Ala4 Hα	Ala5 HN	5.0 Å; Weak

Ala4 Hα	S6 HN	6.0 Å; Very Weak
Ala4 Hα	S6 H1	6.0 Å; Very Weak
Ala4 Hα	S6 H2	6.0 Å; Very Weak
Ala4 HN	Ala5 HN	3.5 Å; Medium
Ala5 Hα	S6 HN	5.0 Å; Weak
Ala5 Hα	S6 H1	6.0 Å; Very Weak
Ala5 Hα	S6 H2	6.0 Å; Very Weak
Ala5 HN	S6 HN	3.5 Å; Medium
S6 HN	S6 H1	3.5 Å; Medium
S6 HN	S6 H2	6.0 Å; Very Weak

φ-angle restraints

Residue	**$^3J_{NH-CH\alpha}$ (Hz)**	**φ-dihedral angle restraint**
Ala3	2.8	-60°± 30°
Ala4	6.1	-60°± 30°

Hydrogen-bond restraints

Donor	**Acceptor**	**H-O Distance**	**N-O Distance**
S6 H1	Ala3 O	1.88[-.3 Å,+.42 Å]	2.88 [-.3 Å,+.32 Å]
S6 NH	S2 O	1.88[-.3 Å,+.42 Å]	2.88 [-.3 Å,+.32 Å]
Ala5 NH	Acetyl1 O	1.88[-.3 Å,+.42 Å]	2.88 [-.3 Å,+.32 Å]

* Represents protons that were not stereospecifically assigned and whose distance restraints were adjusted with standard pseudoatom corrections (Wuthrich, K.; Billeter, M.; Braun, W. *J. Mol. Biol*. **1983**, 169, 949).

Table S4. ^{1}H NMR resonance assignments and chemical shifts (δ ppm) for **3a** in H_2O/D_2O (9:1) at 298K.

Residue	δ (ppm)			
	NH	**Hα**	**Hβ**	**Other**
Ac-X 2	8.14	4.00	1.67	γCH_2 1.37, 1.00; δCH_2 1.83, 1.74; εCH_2 4.37, 4.25; Acetyl Cα 1.92
Ala 3	8.21	3.88	1.28	
Ala 4	7.62	4.13	1.27	
Ala 5	7.87	4.13	1.33	
X 6 $-NH_2$	7.88	4.59	3.26; 3.13	δCH 7.74; NH1 7.29; NH2 7.14

Table S5. ROE-derived distances, $^{3}J_{NH\text{-}CH_\alpha}$ derived j-angle restraints and hydrogen-bond restraints used for calculating the solution structure of **3a** in H_2O/D_2O (9:1) at 298K.

Acetyl1 Hα*	X2 HN	5.0 Å; Medium + 1.5Å correction
Acetyl1 Hα*	Ala3 HN	6.0 Å; Very Weak, no correction
Acetyl1 Hα*	Ala4 HN	6.0 Å; Very Weak, no correction
X2 Hα	Ala4 HN	6.0 Å; Very Weak
X2 HN	Ala5 HN	5.0 Å; Weak
X2 Hα	Ala5 Hβ*	5.0 Å; Strong + 1.5Å correction
X2 HE*	X2 HG*	6.0 Å; Weak (1.0Å correction)
X2 Hα	Ala3 HN	2.7 Å; Strong
X2 Hε*	X6 Hδ2	5.0 Å; Weak
X2 Hβ*	Ala3 HN	6.0 Å; Weak (1.0Å correction)
Ala3 HN	Ala4 HN	3.5 Å; Medium
Ala3 Hα	Ala4 HN	3.5 Å; Medium
Ala3 Hα	Ala5 HN	6.0 Å; Very Weak
Ala3 Hα	X6 Hβ1	6.0 Å; Very Weak
Ala4 Hα	Ala5 HN	2.7 Å; Strong
Ala4 Hα	X6 HN	6.0 Å; Very Weak
Ala4 Hα	X6 H1	6.0 Å; Very Weak
Ala4 Hβ*	Ala5 HN	6.0 Å; Very Weak
Ala4 HN	Ala5 HN	3.5 Å; Medium
Ala5 Hα	X6 HN	6.0 Å; Very Weak
Ala5 Hα	Ala2 Hγ*	6.0 Å; Very Weak
Ala5 Hβ*	X6 HN	6.0 Å; Very Weak
X6 Hα	X6 H1	3.5 Å; Medium
X6 Hα	X6 H2	6.0 Å; Very Weak
X6 HN	X6 H1	5.0 Å; Weak
X6 HN	X6 H2	6.0 Å; Very Weak
X6 Hβ*	X6 Hδ2	5.0 Å; Weak
X6 Hβ1	X6 H1	5.0 Å; Weak
X6 Hβ2	X6 H1	6.0 Å; Very Weak
X6 HN	X6 Hβ1	5.0 Å; Weak
X6 HN	X6 Hβ2	6.0 Å; Very Weak
X6 Hα	X6 Hβ1	3.5 Å; Medium

X6 Hα	X6 Hβ2	5.0 Å; Weak

φ-angle restraints

Residue	$^{3}J_{NH-CH\alpha}$ (Hz)	φ-dihedral angle restraint
X2	4.7	-60°± 30°
Ala3	4.4	-60°± 30°
Ala4	5.8	-60°± 30°
Ala5	5.3	-60°± 30°

Hydrogen-bond restraints

Donor	Acceptor	H-O Distance	N-O Distance
X6 H1	Ala3 O	1.88[-.3 Å,+.42 Å]	2.88 [-.3 Å,+.42 Å]
X6 NH	X2 O	1.88[-.3 Å,+.42 Å]	2.88 [-.3 Å,+.42 Å]
Ala5 NH	Acetyl1 O	1.88[-.3 Å,+.42 Å]	2.88 [-.3 Å,+.42 Å]

* Represents protons that were not stereospecifically assigned and whose distance restraints were adjusted with standard pseudoatom corrections (Wuthrich, K.; Billeter, M.; Braun, W. *J. Mol. Biol.* **1983**, 169, 949).